

1 **Mitochondrial respiratory states and rates:**
2 **Building blocks of mitochondrial physiology Part 1**

3
4 **MitoEAGLE preprint** Version: 2018-03-23(35)

5 Corresponding author: Gnaiger E

6 Co-authors:

7 Aasander Frostner E, Abumrad NA, Acuna-Castroviejo D, Ahn B, Ali SS, Alves MG, Amati
8 F, Aral C, Arandarčikaitė O, Bailey DM, Bajpeyi S, Bakker BM, Bastos Sant'Anna Silva AC,
9 Battino M, Bazil J, Beard DA, Bednarczyk P, Ben-Shachar D, Bergdahl A, Bernardi P,
10 Bishop D, Blier PU, Boetker HE, Boros M, Borsheim E, Borutaitė V, Bouillaud F, Boutbir J,
11 Breton S, Brown DA, Brown GC, Brown RA, Brozinick JT, Buettner GR, Burtscher J,
12 Calabria E, Calbet JA, Calzia E, Cannon DT, Canto AC, Cardoso LHD, Carvalho E, Casado
13 Pinna M, Cassina AM, Cavalcanti-de-Albuquerque JP, Cervinkova Z, Chang SC, Chaurasia
14 B, Chen Q, Chicco AJ, Chinopoulos C, Clementi E, Coen PM, Coker RH, Collin A,
15 Crisóstomo L, Darveau CA, Das AM, Dash RK, Davis MS, De Palma C, Dembinska-Kiec A,
16 Dias TR, Distefano G, Doerrier C, Drahotka Z, Dubouchaud H, Duchon MR, Dumas JF,
17 Durham WJ, Dymkowska D, Dyrstad SE, Dzialowski EM, Ehinger J, Elmer E, Endlicher R,
18 Engin AB, Fell DA, Ferko M, Ferreira JCB, Ferreira R, Fessel JP, Filipovska A, Fisar Z,
19 Fischer M, Fisher G, Fisher JJ, Fornaro M, Galkin A, Gan Z, Garcia-Roves PM, Garcia-Souza
20 LF, Garlid KD, Garrabou G, Garten A, Gastaldelli A, Genova ML, Giovarelli M, Gonzalez-
21 Armenta JL, Gonzalo H, Goodpaster BH, Gorr TA, Gourlay CW, Granata C, Grefte S, Haas
22 CB, Haavik J, Haendeler J, Hamann A, Han J, Hancock CR, Hand SC, Hargreaves I, Harrison
23 DK, Hellgren KT, Hepple RT, Hernansanz-Agustin P, Hickey AJ, Hoel F, Holland OJ,
24 Holloway GP, Hoppel CL, Houstek J, Hunger M, Iglesias-Gonzalez J, Irving BA, Iyer S,
25 Jackson CB, Jadiya P, Jang DH, Jang YC, Jansen-Dürr P, Jespersen NR, Jha RK, Jurk D,
26 Kaambre T, Kaczor JJ, Kainulainen H, Kandel SM, Kane DA, Kappler L, Karabatsiakakis A,
27 Karkucinska-Wieckowska A, Keijer J, Keppner G, Khamoui AV, Klingenspor M, Komlodi T,
28 Koopman WJH, Kopitar-Jerala N, Kowaltowski AJ, Krajcova A, Krako Jakovljevic N, Kuang
29 J, Kucera O, Kwak HB, Kwast K, Labieniec-Watala M, Lai N, Land JM, Lane N, Laner V,
30 Lanza IR, Larsen TS, Lavery GG, Lee HK, Leuwenburgh C, Lemieux H, Lerfall J, Li PA,
31 Liu J, Lucchinetti E, Macedo MP, MacMillan-Crow LA, Makrecka-Kuka M, Malik A,
32 Markova M, Martin DS, Mazat JP, McKenna HT, Menze MA, Meszaros AT, Methner A,
33 Michalak S, Moellering DR, Moiso N, Molina AJA, Montaigne D, Moreau K, Moore AL,
34 Moreira BP, Mracek T, Muntane J, Muntean DM, Murray AJ, Nair KS, Nemeš M, Neuffer
35 PD, Neuzil J, Newsom S, Nozickova K, O'Gorman D, Oliveira MF, Oliveira MT, Oliveira PF,
36 Oliveira PJ, Orynbayeva Z, Osiewacz HD, Pak YK, Pallotta ML, Palmeira CM, Parajuli N,
37 Passos JF, Patel HH, Pecina P, Pelna D, Pereira da Silva Grilo da Silva F, Pesta D, Petit
38 PX, Pettersen IK, Pichaud N, Piel S, Pietka TA, Pino MF, Pirkmajer S, Porter C, Porter RK,
39 Pranger F, Prochownik EV, Pulnilkunnit T, Puskarich MA, Puurand M, Radenkovic F, Radi
40 R, Ramzan R, Rattan S, Reboledo P, Renner-Sattler K, Robinson MM, Roden M, Rohlena J,
41 Rolo AP, Ropelle ER, Røslund GV, Rossiter HB, Rybacka-Mossakowska J, Saada A, Safaei
42 Z, Salin K, Salvadego D, Sandi C, Sazanov LA, Scatena R, Schartner M, Scheibye-Knudsen
43 M, Schilling JM, Schlattner U, Schönfeld P, Schwarzer C, Scott GR, Shabalina IG, Sharma P,
44 Sharma V, Shevchuk I, Siewiera K, Silber AM, Silva AM, Sims CA, Singer D, Skolik R,
45 Smenes BT, Smith J, Soares FAA, Sobotka O, Sokolova I, Sonkar VK, Sparagna GC, Sparks
46 LM, Spinazzi M, Stankova P, Stary C, Stier A, Stocker R, Sumbalova Z, Suravajhala P,
47 Swerdlow RH, Swiniuch D, Tanaka M, Tandler B, Tavernarakis N, Tepp K, Thyfault JP,
48 Tomar D, Towheed A, Tretter L, Trifunovic A, Trivigno C, Tronstad KJ, Trougakos IP,
49 Tyrrell DJ, Urban T, Valentine JM, Velika B, Vendelin M, Vercesi AE, Victor VM, Vieyra A
50 Villena JA, Vitorino RMP, Vogt S, Volani C, Votion DM, Vujacic-Mirski K, Wagner BA,
51 Ward ML, Warnsmann V, Wasserman DH, Watala C, Wei YH, Wieckowski MR, Williams

C, Wohlgemuth SE, Wohlwend M, Wolff J, Wüst RCI, Yokota T, Zablocki K, Zaugg K,
Zaugg M, Zhang Y, Zischka H, Zorzano A

Updates and discussion:

http://www.mitoeagle.org/index.php/MitoEAGLE_preprint_2018-02-08

Correspondence: Gnaiger E

Chair COST Action CA15203 MitoEAGLE – <http://www.mitoeagle.org>

*Department of Visceral, Transplant and Thoracic Surgery, D. Swarovski Research
Laboratory, Medical University of Innsbruck, Innrain 66/4, A-6020 Innsbruck, Austria*

Email: mitoeagle@i-med.ac.at

Tel: +43 512 566796, Fax: +43 512 566796 20

Abstract - Executive summary

1. Introduction – Box 1: In brief: Mitochondria and Bioblasts

2. Oxidative phosphorylation and coupling states in mitochondrial preparations

Mitochondrial preparations

2.1. Respiratory control and coupling

The steady-state

Specification of biochemical dose

Phosphorylation, P_{\gg} , and P_{\gg}/O_2 ratio

Control and regulation

Respiratory control and response

Respiratory coupling control and ET-pathway control

Coupling

Uncoupling

2.2. Coupling states and respiratory rates

Respiratory capacities in coupling control states

LEAK, OXPHOS, ET, ROX

Quantitative relations

2.3. Classical terminology for isolated mitochondria

States 1–5

3. Normalization: fluxes and flows

3.1. Normalization: system or sample

Flow per system, I

Extensive quantities

Size-specific quantities – Box 2: Metabolic fluxes and flows: vectorial and scalar

3.2. Normalization for system-size: flux per chamber volume

System-specific flux, J_{V,O_2}

3.3. Normalization: per sample

Sample concentration, C_{mX}

Mass-specific flux, $J_{O_2/mX}$

Number concentration, C_{NX}

Flow per object, $I_{O_2/X}$

3.4. Normalization for mitochondrial content

Mitochondrial concentration, C_{mtE} , and mitochondrial markers

Mitochondria-specific flux, $J_{O_2/mtE}$

3.5. Evaluation of mitochondrial markers

3.6. Conversion: units

4. Conclusions

References

104 **Abstract** As the knowledge base and importance of mitochondrial physiology to human health
105 expands, the necessity for harmonizing the terminology concerning mitochondrial respiratory
106 states and rates has become increasingly apparent. The chemiosmotic theory establishes the
107 mechanism of energy transformation and coupling in oxidative phosphorylation. The unifying
108 concept of the protonmotive force provides the framework for developing a consistent
109 theoretical foundation of mitochondrial physiology and bioenergetics. We follow IUPAC
110 guidelines on terminology in physical chemistry, extended by considerations on open systems
111 and irreversible thermodynamics. The concept-driven constructive terminology incorporates
112 the meaning of each quantity and aligns concepts and symbols to the nomenclature of classical
113 bioenergetics. In the frame of COST Action MitoEAGLE open to global bottom-up input, we
114 endeavour to provide a balanced view on mitochondrial respiratory control and a critical
115 discussion on reporting data of mitochondrial respiration in terms of metabolic flows and fluxes.
116 Uniform standards for evaluation of respiratory states and rates will ultimately support the
117 development of databases of mitochondrial respiratory function in species, tissues, and cells.
118 Clarity of concept and consistency of nomenclature facilitate effective transdisciplinary
119 communication, education, and ultimately further discovery.

120

121 *Keywords:* Mitochondrial respiratory control, coupling control, mitochondrial
122 preparations, protonmotive force, uncoupling, oxidative phosphorylation, OXPHOS,
123 efficiency, electron transfer, ET; proton leak, LEAK, residual oxygen consumption, ROX, State
124 2, State 3, State 4, normalization, flow, flux, O₂

125

126 **Executive summary**

127

- 128 1. In view of the broad implications for health care, mitochondrial researchers face an
129 increasing responsibility to disseminate their fundamental knowledge and novel
130 discoveries to a wide range of stakeholders and scientists beyond the group of
131 specialists. This requires implementation of a commonly accepted terminology
132 within the discipline and standardization in the translational context. Authors,
133 reviewers, journal editors, and lecturers are challenged to collaborate with the aim
134 to harmonize the nomenclature in the growing field of mitochondrial physiology
135 and bioenergetics.
- 136 2. Aerobic respiration depends on the coupling of phosphorylation (ADP → ATP) to O₂
137 flux in catabolic reactions. Coupling in oxidative phosphorylation is mediated by
138 translocation of protons across the inner mitochondrial membrane through proton
139 pumps generating or utilizing the protonmotive force, that is measured between the
140 mitochondrial matrix and intermembrane compartment. Compartmental coupling
141 distinguishes vectorial oxidative phosphorylation from glycolytic fermentation as
142 the counterpart of cellular core energy metabolism (**Figure 1**).
- 143 3. To exclude fermentation and other cytosolic interactions from exerting an effect on the
144 analysis of mitochondrial metabolism, the barrier function of the plasma membrane
145 must be disrupted. Selective removal or permeabilization of the plasma membrane
146 yields mitochondrial preparations—including isolated mitochondria, tissue and
147 cellular preparations—with structural and functional integrity. Then, extra-
148 mitochondrial concentrations of fuel substrates, ADP, ATP, inorganic phosphate,
149 and cations including H⁺ can be controlled to determine mitochondrial function
150 under a set of conditions defined as coupling control states. A concept-driven
151 terminology of bioenergetics explicitly incorporates in its terms and symbols
152 information on the nature of respiratory states that makes the technical terms readily
153 recognized and more easy to understand.

154 **Figure 1. Mitochondrial**
 155 **respiration is the oxidation of fuel**
 156 **substrates (electron donors) and**
 157 **reduction of O₂ catalysed by the**
 158 **electron transfer system, ETS: (a)**
 159 **catabolic respiration (including**
 160 **non-mitochondrial oxidation**
 161 **reactions, b), and oxygen balance**
 162 **of internal (c) and external (d)**
 163 **respiration**

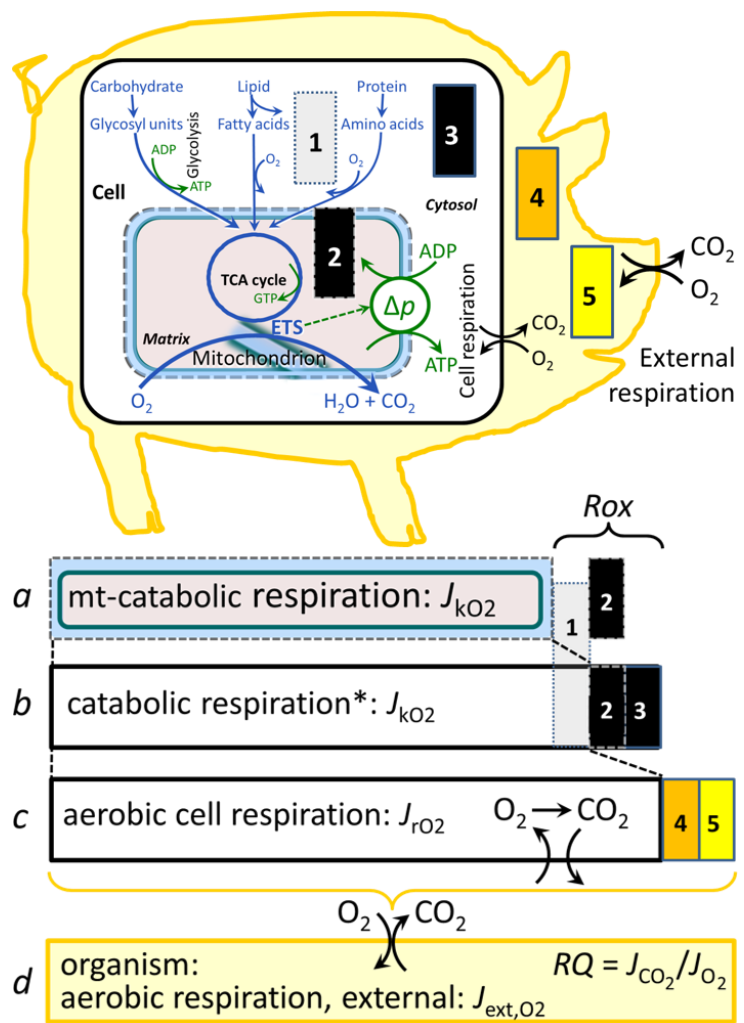
164 All chemical reactions, r , that
 165 consume O₂ in the cells of an
 166 organism, contribute to cell
 167 respiration, J_{rO_2} . ❶ Non-
 168 non-mitochondrial O₂ consumption
 169 by catabolic reactions, particularly
 170 peroxisomal oxidases; ❷
 171 mitochondrial residual oxygen
 172 consumption, R_{ox} , after blocking
 173 the ETS; ❸ non-mitochondrial R_{ox} ;
 174 ❹ extracellular O₂ consumption; ❺
 175 aerobic microbial respiration. Bars
 176 are not at a quantitative scale.

177 **a Mitochondrial catabolic**
 178 **respiration**, J_{kO_2} , is the O₂
 179 consumption by the
 180 mitochondrial ETS maintaining
 181 the protonmotive force, Δp . J_{kO_2}
 182 excludes R_{ox} .

183 **b Catabolic respiration** is the O₂ consumption associated with catabolic pathways in the cell,
 184 including peroxisomal oxidation reactions (❶) in addition to mitochondrial catabolism (*
 185 The reactions k have to be defined specifically for *a* and *b*.)

186 **c Aerobic cell respiration**, J_{rO_2} , takes into account internal O₂-consuming reactions, r ,
 187 including catabolic respiration and R_{ox} . Internal respiration of an organism includes
 188 extracellular O₂ consumption (❹) and aerobic respiration by the microbiome (❺).
 189 Respiration is distinguished from fermentation by: (1) External electron acceptors for the
 190 maintenance of redox balance, whereas fermentation is characterized by an internal electron
 191 acceptor produced in intermediary metabolism. In aerobic cell respiration, redox balance is
 192 maintained by O₂ as the electron acceptor. (2) Compartmental coupling in vectorial oxidative
 193 phosphorylation, in contrast to exclusively scalar substrate-level phosphorylation in
 194 fermentation.

195 **d External respiration** balances internal respiration at steady-state. O₂ is transported from the
 196 environment across the respiratory cascade (circulation between tissues and diffusion across
 197 cell membranes) to the intracellular compartment, while bicarbonate and CO₂ are transported
 198 in reverse to the extracellular milieu and the organismic environment. Hemoglobin provides
 199 the molecular paradigm for the combination of O₂ and CO₂ exchange, as do lungs and gills
 200 on the morphological level. The respiratory quotient, RQ , is the molar CO₂/O₂ exchange
 201 ratio; when combined with the respiratory nitrogen quotient, N/O₂ (mol N given off per mol
 202 O₂ consumed), the RQ reflects the proportion of carbohydrate, lipid and protein utilized in
 203 cell respiration during aerobically balanced steady-states.
 204



- 205 4. Mitochondrial coupling states are defined according to the control of respiratory oxygen
 206 flux by the protonmotive force. Capacities of oxidative phosphorylation and
 207 electron transfer are measured at kinetically saturating concentrations of fuel
 208 substrates, ADP and inorganic phosphate, or at optimal uncoupler concentrations,
 209 respectively. Respiratory capacity is a measure of the upper bound of the rate of
 210 respiration, depends on the substrate type undergoing oxidation, and provides
 211 reference values for the diagnosis of health and disease, and for evaluation of the
 212 effects of Evolutionary background, Age, Gender and sex, Lifestyle and
 213 Environment (EAGLE).
- 214 5. Incomplete ~~tightness~~ of coupling, *i.e.*, some degree of uncoupling relative to the
 215 substrate-dependent coupling stoichiometry, is a characteristic of energy-
 216 transformations across membranes. Uncoupling is caused by a variety of
 217 physiological, pathological, toxicological, pharmacological and environmental
 218 conditions that exert an influence not only on the proton leak and cation cycling,
 219 but also on proton slip within the proton pumps and the structural integrity of the
 220 mitochondria. A more loosely coupled state is induced by stimulation of
 221 mitochondrial superoxide formation and the bypass of proton pumps. In addition,
 222 uncoupling by application of protonophores represents an experimental
 223 intervention for the transition from a well-coupled to the noncoupled state of
 224 mitochondrial respiration.
- 225 6. Respiratory oxygen consumption rates have to be carefully normalized to enable meta-
 226 analytic studies beyond the specific question of a particular experiment. Therefore,
 227 all raw data should be published in a supplemental table or open access data
 228 repository. Normalization of rates for the volume of the experimental chamber (the
 229 measuring system) is distinguished from normalization for: (1) the volume or mass
 230 of the experimental sample; (2) the number of objects (cells, organisms); and (3)
 231 the concentration of mitochondrial markers in the chamber.
- 232 7. The consistent use of terms and symbols will facilitate transdisciplinary communication
 233 and support further developments of a database on bioenergetics and mitochondrial
 234 physiology. The present considerations are focused on studies with mitochondrial
 235 preparations. These will be extended in a series of reports on pathway control of
 236 mitochondrial respiration, the protonmotive force, respiratory states in intact cells,
 237 and harmonization of experimental procedures.
 238

241 **Box 1: In brief – Mitochondria and Bioblasts**

242 *‘For the physiologist, mitochondria afforded the first opportunity for an*
 243 *experimental approach to structure-function relationships, in particular those*
 244 *involved in active transport, vectorial metabolism, and metabolic control*
 245 *mechanisms on a subcellular level’ (Ernster and Schatz 1981).*

246 **Mitochondria** are the oxygen-consuming electrochemical generators evolved from
 247 endosymbiotic bacteria (Margulis 1970; Lane 2005). They were described by Richard Altmann
 248 (1894) as ‘bioblasts’, which include not only the mitochondria as presently defined, but also
 249 symbiotic and free-living bacteria. The word ‘mitochondria’ (Greek mitos: thread; chondros:
 250 granule) was introduced by Carl Benda (1898).

251 Mitochondria are dynamic networks contained within eukaryotic cells morphologically
 252 enclosed by a double membrane. The mitochondrial inner membrane (mtIM) shows dynamic
 253 tubular to disk-shaped cristae that separate the mitochondrial matrix, *i.e.*, the negatively charged
 254 internal mitochondrial compartment, from the intermembrane space; the latter being positively
 255 charged and enclosed by the mitochondrial outer membrane (mtOM). The mtIM contains the
 256 non-bilayer phospholipid cardiolipin, which is not present in any other eukaryotic cellular

257 membrane. Cardiolipin stabilizes and promotes the formation of respiratory supercomplexes
 258 (SC I_nIII_nIV_n), which are supramolecular assemblies based upon specific, though dynamic
 259 interactions between individual respiratory complexes (Greggio *et al.* 2017; Lenaz *et al.* 2017).
 260 Membrane fluidity exerts an influence on functional properties of proteins incorporated in the
 261 membranes (Waczulikova *et al.* 2007). In addition to mitochondrial movement along
 262 microtubules, mitochondrial morphology can change in response to energy requirements of the
 263 cell via processes known as fusion and fission, through which mitochondria communicate
 264 within a network. Intracellular stress factors may cause shrinking or swelling of the
 265 mitochondrial matrix, which can ultimately result in permeability transition.

266 Mitochondria are the structural and functional elements of cell respiration. Mitochondrial
 267 respiration is the reduction of oxygen by electron transfer coupled to electrochemical proton
 268 translocation across the mtIM. In the process of oxidative phosphorylation (OXPHOS), the
 269 catabolic reaction of oxygen consumption is electrochemically coupled to the transformation of
 270 energy in the form of adenosine triphosphate (ATP; Mitchell 1961, 2011). Mitochondria are the
 271 powerhouses of the cell which contain the machinery of the OXPHOS-pathways, including
 272 transmembrane respiratory complexes (proton pumps with FMN, Fe-S and cytochrome *b*, *c*,
 273 *aa*₃ redox systems); alternative dehydrogenases and oxidases; the coenzyme ubiquinone (Q);
 274 F-ATPase or ATP synthase; the enzymes of the tricarboxylic acid cycle, fatty acid and
 275 aminoacid oxidation; transporters of ions, metabolites and co-factors; iron/sulphur cluster
 276 synthesis; and mitochondrial kinases related to energy transfer pathways. The mitochondrial
 277 proteome comprises over 1,200 proteins (Calvo *et al.* 2015; 2017), mostly encoded by nuclear
 278 DNA (nDNA), with a variety of functions, many of which are relatively well known (*e.g.*,
 279 proteins regulating mitochondrial biogenesis or apoptosis), while others are still under
 280 investigation, or need to be identified (*e.g.*, alanine transporter). Only lately it is possible to use
 281 the mammalian mitochondrial proteome to discover and characterize the genetic basis of
 282 mitochondrial diseases (Williams *et al.* 2016; Palmfeldt and Bross 2017).

283 There is a constant crosstalk between mitochondria and the other cellular components.
 284 The crosstalk between mitochondria and endoplasmic reticulum is involved in the regulation of
 285 calcium homeostasis, cell division, autophagy, differentiation, and anti-viral signaling (Murley
 286 and Nunnari 2016). Mitochondria contribute to the formation of peroxisomes, which are hybrids
 287 of mitochondrial and ER-derived precursors (Sugiura *et al.* 2017). Cellular mitochondrial
 288 homeostasis (mitostasis) is maintained through regulation at both the transcriptional and post-
 289 translational level. Cell signalling modules contribute to homeostatic regulation throughout the
 290 cell cycle or even cell death by activating proteostatic modules (*e.g.*, the ubiquitin-proteasome
 291 and autophagy-lysosome/vacuole pathways; specific proteases like LON) and genome stability
 292 modules in response to varying energy demands and stress cues (Quiros *et al.* 2016).
 293 Acetylation is a post-translational modification capable of influencing the bioenergetic
 294 response, with clinically significant implications for health and disease (Carrico *et al.* 2018).
 295 Mitochondria can traverse cell boundaries in a process known as horizontal mitochondrial
 296 transfer ~~between cells~~ (Torralba *et al.* 2016).

297 Mitochondria typically maintain several copies of their own circular genome known as
 298 mitochondrial DNA (mtDNA; hundred to thousands per cell; Cummins 1998), which is
 299 maternally inherited. Biparental mitochondrial inheritance is documented in mammals, birds,
 300 fish, reptiles and invertebrate groups, and is even the norm in bivalves (Breton *et al.* 2007;
 301 White *et al.* 2008). The mitochondrial genome of the angiosperm *Amborella* contains a record
 302 of six mitochondrial genome equivalents acquired by horizontal transfer of entire genomes, two
 303 from angiosperms, three from algae and one from mosses (Rice *et al.* 2016). However, some
 304 organisms such as *Cryptosporidium* species have morphologically and functionally reduced
 305 mitochondria without DNA (Liu *et al.* 2016). mtDNA is compact (16.5 kB in humans) and
 306 encodes 13 protein subunits of the transmembrane respiratory Complexes CI, CIII, CIV and F-
 307 ATPase, 22 tRNAs, and two RNAs. Additional gene content has been suggested to include

308 microRNAs, piRNA, smithRNAs, repeat associated RNA, and even additional proteins (Duarte
309 *et al.* 2014; Lee *et al.* 2015; Cobb *et al.* 2016). The mitochondrial genome requires nuclear-
310 encoded mitochondrially targeted proteins for its maintenance and expression (Rackham *et al.*
311 2012).

312 Mitochondrial dysfunction is associated with a wide variety of genetic and degenerative
313 diseases. Robust mitochondrial function is supported by physical exercise and caloric balance,
314 and is central for sustained metabolic health throughout life. Therefore, a more consistent
315 presentation of mitochondrial physiology will improve our understanding of the etiology of
316 disease, the diagnostic repertoire of mitochondrial medicine, with a focus on protective
317 medicine, lifestyle and healthy aging.

318 Abbreviation: mt, as generally used in mtDNA. Mitochondrion is singular and
319 mitochondria is plural.

321

322

323 1. Introduction

324

325 Mitochondria are the powerhouses of the cell with numerous physiological, molecular,
326 and genetic functions (**Box 1**). Every study of mitochondrial health and disease is faced with
327 **E**volution, **A**ge, **G**ender and sex, **L**ifestyle, and **E**nvironment (EAGLE) as essential background
328 conditions intrinsic to the individual patient or subject, cohort, species, tissue and to some extent
329 even cell line. As a large and coordinated group of laboratories and researchers, the mission of
330 the global MitoEAGLE Network is to generate the necessary scale, type, and quality of
331 consistent data sets and conditions to address this intrinsic complexity. Harmonization of
332 experimental protocols and implementation of a quality control and data management system
333 are required to interrelate results gathered across a spectrum of studies and to generate a
334 rigorously monitored database focused on mitochondrial respiratory function. In this way,
335 researchers within the same and across different disciplines can compare findings across
336 traditions and generations to clearly defined and accepted international standards.

337 Reliability and comparability of quantitative results depend on the accuracy of
338 measurements under strictly-defined conditions. A conceptual framework is required to warrant
339 meaningful interpretation and comparability of experimental outcomes carried out by research
340 groups at different institutes. With an emphasis on quality of research, collected data can be
341 useful far beyond the specific question of a particular experiment. Standardization and
342 homogenization of terminology, methodology, and data sets could lead to the development of
343 open-access databases such as those that have been developed for National Institutes of Health
344 sponsored research in genetics, proteomics, and metabolomics. Enabling meta-analytic studies
345 is the most economic way of providing robust answers to biological questions (Cooper *et al.*
346 2009). Vague or ambiguous jargon can lead to confusion and may relegate valuable signals to
347 wasteful noise. For this reason, measured values must be expressed in standard units for each
348 parameter used to define mitochondrial respiratory function. Harmonization of nomenclature
349 and definition of technical terms are essential to improve the awareness of the intricate meaning
350 of current and past scientific vocabulary, for documentation and integration into databases in
351 general, and quantitative modelling in particular (Beard 2005). The focus on coupling states
352 and fluxes through metabolic pathways of aerobic energy transformation in mitochondrial
353 preparations is a first step in the attempt to generate a conceptually-oriented nomenclature in
354 bioenergetics and mitochondrial physiology. Coupling states of intact cells, the protonmotive
355 force, and respiratory control by fuel substrates and specific inhibitors of respiratory enzymes
356 will be reviewed in subsequent communications.

357

358

2. Oxidative phosphorylation and coupling states in mitochondrial preparations

‘Every professional group develops its own technical jargon for talking about matters of critical concern ... People who know a word can share that idea with other members of their group, and a shared vocabulary is part of the glue that holds people together and allows them to create a shared culture’ (Miller 1991).

Mitochondrial preparations are defined as either isolated mitochondria, or tissue and cellular preparations in which the barrier function of the plasma membrane is disrupted. Since this entails the loss of cell viability, mitochondrial preparations are not studied *in vivo*. In contrast to isolated mitochondria and tissue homogenate preparations, mitochondria in permeabilized tissues and cells are *in situ* relative to the plasma membrane. The plasma membrane separates the intracellular compartment including the cytosol, nucleus, and organelles from the environment of the cell. The plasma membrane consists of a lipid bilayer with embedded proteins and attached organic molecules that collectively control the selective permeability of ions, organic molecules, and particles across the cell boundary. The intact plasma membrane prevents the passage of many water-soluble mitochondrial substrates and inorganic ions—such as succinate, adenosine diphosphate (ADP) and inorganic phosphate (P_i), that must be controlled at kinetically-saturating concentrations for the analysis of respiratory capacities; this limits the scope of investigations into mitochondrial respiratory function in intact cells (**Figure 2A**).

The cholesterol content of the plasma membrane is high compared to mitochondrial membranes. Therefore, mild detergents—such as digitonin and saponin—can be applied to selectively permeabilize the plasma membrane by interaction with cholesterol and allow free exchange of organic molecules and inorganic ions between the cytosol and the immediate cell environment, while maintaining the integrity and localization of organelles, cytoskeleton, and the nucleus. Application of optimum concentrations of permeabilization agents (mild detergents or toxins) leads to washout of cytosolic marker enzymes—such as lactate dehydrogenase—and results in the complete loss of cell viability, tested by nuclear staining using membrane-impermeable dyes, while mitochondrial function remains intact. Respiration of isolated mitochondria remains unaltered after the addition of low concentrations of digitonin or saponin. In addition to mechanical cell disruption during homogenization of tissue, permeabilization agents may be applied to ensure permeabilization of all cells. Suspensions of cells permeabilized in the respiration chamber and crude tissue homogenates contain all components of the cell at highly dilute concentrations. All mitochondria are retained in chemically-permeabilized mitochondrial preparations and crude tissue homogenates. In the preparation of isolated mitochondria, the cells or tissues are homogenized, and the mitochondria are separated from other cell fractions and purified by differential centrifugation, entailing the loss of a fraction of the total mitochondrial content. Typical mitochondrial recovery ranges from 30% to 80%, or less if mitochondria are purified further by, *e.g.*, sucrose gradients. Maximization of the purity of isolated mitochondria may compromise not only the mitochondrial yield but also the structural and functional integrity. Therefore, protocols to isolate mitochondria need to be optimized according to each study. The term mitochondrial preparation does **not** include further fractionation of mitochondrial components, **neither** submitochondrial particles.

2.1. Respiratory control and coupling

Respiratory coupling control states are established in studies of mitochondrial preparations to obtain reference values for various output variables. Physiological conditions *in vivo* deviate from these experimentally obtained states. Since kinetically-saturating concentrations, *e.g.*, of ADP or oxygen (O_2 ; dioxygen), may not apply to physiological intracellular conditions, relevant information is obtained in studies of kinetic responses to

410 variations in [ADP] or [O₂] in the range between kinetically-saturating concentrations and
 411 anoxia (Gnaiger 2001).

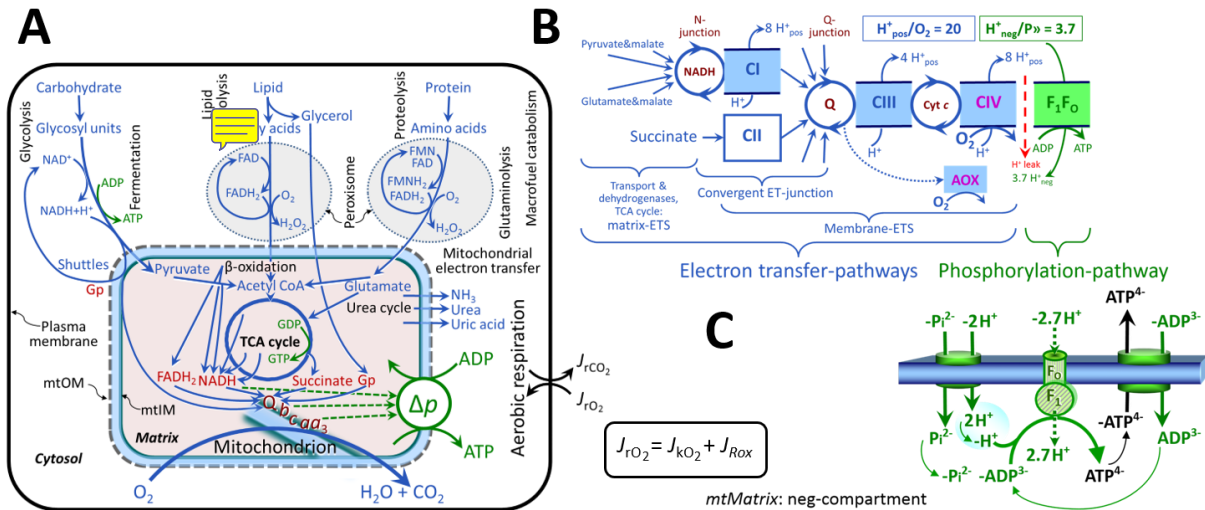
412 **The steady-state:** Mitochondria represent a thermodynamically open system in non-
 413 equilibrium states of biochemical energy transformation. State variables (protonmotive force;
 414 redox states) and metabolic *rates* (fluxes) are measured in defined mitochondrial respiratory
 415 *states*. Steady-states can be obtained only in open systems, in which changes by *internal*
 416 transformations, *e.g.*, O₂ consumption, are instantaneously compensated for by *external* fluxes,
 417 *e.g.*, O₂ supply, preventing a change of O₂ concentration in the system (Gnaiger 1993b).
 418 Mitochondrial respiratory states monitored in closed systems satisfy the criteria of pseudo-
 419 steady states for limited periods of time, when changes in the system (concentrations of O₂, fuel
 420 substrates, ADP, P_i, H⁺) do not exert significant effects on metabolic fluxes (respiration,
 421 phosphorylation). Such pseudo-steady states require respiratory media with sufficient buffering
 422 capacity and substrates maintained at kinetically-saturating concentrations, and thus depend on
 423 the kinetics of the processes under investigation.

424 **Specification of biochemical dose:** Substrates, uncouplers, inhibitors, and other
 425 chemical reagents are titrated to dissect mitochondrial function. Nominal concentrations of
 426 these substances are usually reported as initial amount of substance concentration [mol·L⁻¹] in
 427 the incubation medium. When aiming at the measurement of kinetically saturated processes—
 428 such as OXPHOS-capacities, the concentrations for substrates can be chosen according to the
 429 apparent equilibrium constant, K_m' . In the case of hyperbolic kinetics, only 80% of maximum
 430 respiratory capacity is obtained at a substrate concentration of four times the K_m' , whereas
 431 substrate concentrations of 5, 9, 19 and 49 times the K_m' are theoretically required for reaching
 432 83%, 90%, 95% or 98% of the maximal rate (Gnaiger 2001). Other reagents are chosen to
 433 inhibit or alter some processes. The amount of these chemicals in an experimental incubation
 434 is selected to maximize effect, avoiding unacceptable off-target consequences that would
 435 adversely affect the data being sought. Specifying the amount of substance in an incubation as
 436 nominal concentration in the aqueous incubation medium can be ambiguous (Doskey *et al.*
 437 2015), particularly for lipophilic substances (oligomycin, uncouplers, permeabilization agents)
 438 or cations (TPP⁺; fluorescent dyes such as safranin, TMRM), which accumulate in biological
 439 membranes or in the mitochondrial matrix. For example, a dose of digitonin of 8 fmol·cell⁻¹ (10
 440 pg·cell⁻¹; 10 μg·10⁻⁶ cells) is optimal for permeabilization of endothelial cells, and the
 441 concentration in the incubation medium has to be adjusted according to the cell density applied
 442 (Doerrier *et al.* 2018).

443 Generally, dose/exposure can be specified per unit of biological sample, *i.e.*, (nominal
 444 moles of xenobiotic)/(number of cells) [mol·cell⁻¹] or, as appropriate, per mass of biological
 445 sample [mol·kg⁻¹]. This approach to specification of dose/exposure provides a scalable
 446 parameter that can be used to design experiments, help interpret a wide variety of experimental
 447 results, and provide absolute information that allows researchers worldwide to make the most
 448 use of published data (Doskey *et al.* 2015).

449 **Phosphorylation, P_», and P_»/O₂ ratio:** *Phosphorylation* in the context of OXPHOS is
 450 defined as phosphorylation of ADP by P_i to form ATP. On the other hand, the term
 451 phosphorylation is used generally in many contexts, *e.g.*, protein phosphorylation. This justifies
 452 consideration of a symbol more discriminating and specific than P as used in the P/O ratio
 453 (phosphate to atomic oxygen ratio), where P indicates phosphorylation of ADP to ATP or GDP
 454 to GTP (**Figure 2**). We propose the symbol P_» for the endergonic (uphill) direction of
 455 phosphorylation ADP→ATP, and likewise the symbol P_« for the corresponding exergonic
 456 (downhill) hydrolysis ATP→ADP (**Figure 3**). P_» refers mainly to electrontransfer
 457 phosphorylation but may also involve substrate-level phosphorylation as part of the
 458 tricarboxylic acid (TCA) cycle (succinyl-CoA ligase; phosphoglycerate kinase) and
 459 phosphorylation of ADP catalyzed by pyruvate kinase, and of GDP phosphorylated by
 460 phosphoenolpyruvate carboxykinase. Transphosphorylation is performed by adenylate kinase,

461 creatine kinase, hexokinase and nucleoside diphosphate kinase. In isolated mammalian
 462 mitochondria, ATP production catalyzed by adenylate kinase ($2 \text{ ADP} \leftrightarrow \text{ATP} + \text{AMP}$) proceeds
 463 without fuel substrates in the presence of ADP (Komlódi and Tretter 2017). Kinase cycles are
 464 involved in intracellular energy transfer and signal transduction for regulation of energy flux.
 465



466

467

Figure 2. Cell respiration and oxidative phosphorylation (OXPHOS)

Mitochondrial respiration is the oxidation of fuel substrates (electron donors) with electron transfer to O_2 as the electron acceptor. For explanation of symbols see also **Figure 1**.

468

469

470

471

472

473

474

475

476

477

478

479

480

481

482

483

484

485

486

487

488

489

490

491

492

493

494

495

496

497

498

(A) Respiration in intact cells: Extra-mitochondrial catabolism of macrofuels or uptake of small molecules by the cell provides the *mitochondrial* fuel substrates. Many fuel substrates are catabolized to acetyl-CoA or glutamate, and further electron transfer reduces nicotinamide adenine dinucleotide to NADH or flavin adenine dinucleotide to FADH_2 . In aerobic respiration, electron transfer is coupled to the phosphorylation of ADP to ATP, with energy transformation mediated by the protonmotive force, Δp . Anabolic reactions are linked to catabolism, both by ATP as the intermediary energy currency and by small organic precursor molecules as building blocks for biosynthesis (not shown). Glycolysis involves substrate-level phosphorylation of ADP to ATP in fermentation without utilization of O_2 . In contrast, extra-mitochondrial oxidation of fatty acids and amino acids proceeds partially in peroxisomes without coupling to ATP production: acyl-CoA oxidase catalyzes the oxidation of FADH_2 with electron transfer to O_2 ; amino acid oxidases oxidize flavin mononucleotide FMNH_2 or FADH_2 . Coenzyme Q, Q, and the cytochromes *b*, *c*, and *aa*₃ are redox systems of the mitochondrial inner membrane, mtIM. Dashed arrows indicate the connection between the redox proton pumps (respiratory Complexes CI, CIII and CIV) and the transmembrane Δp . Mitochondrial outer membrane, mtOM; glycerol-3-phosphate, Gp; tricarboxylic acid cycle, TCA cycle.

(B) Respiration in mitochondrial preparations: The mitochondrial electron transfer system (ETS) is fuelled by diffusion and transport of substrates across the mitochondrial outer and inner membrane and consists of the matrix-ETS and membrane-ETS. ET-pathways are coupled to the phosphorylation-pathway. ET-pathways converge at the N-junction and Q-junction. Additional arrows indicate electron entry into the Q-junction through electron transferring flavoprotein, glycerophosphate dehydrogenase, dihydro-orotate dehydrogenase, choline dehydrogenase, and sulfide-ubiquinone oxidoreductase. The dotted arrow indicates the branched pathway of oxygen consumption by alternative quinol oxidase (AOX). The $\text{H}^+_{\text{pos}}/\text{O}_2$ ratio is the outward proton flux from the matrix space to the positively (pos) charged vesicular compartment, divided by catabolic O_2 flux in the NADH-pathway. The $\text{H}^+_{\text{neg}}/\text{P}$ ratio is the inward proton flux from the inter-membrane space to the negatively (neg) charged matrix space, divided by the flux of phosphorylation of ADP to ATP. These are not fixed stoichiometries due to ion leaks and proton slip.

499 **(C)** Phosphorylation-pathway catalyzed by the proton pump F_1F_0 -ATPase (F-ATPase, ATP
 500 synthase), adenine nucleotide translocase, and inorganic phosphate transporter. The H^+_{neg}/P_{\gg}
 501 stoichiometry is the sum of the coupling stoichiometry in the F-ATPase reaction ($-2.7 H^+_{pos}$
 502 from the positive intermembrane space, $2.7 H^+_{neg}$ to the matrix, *i.e.*, the negative compartment)
 503 and the proton balance in the translocation of ADP^{3-} , ATP^{4-} and P_i^{2-} . Modified from (B)
 504 Lemieux *et al.* (2017) and (C) Gnaiger (2014).
 505

506 The P_{\gg}/O_2 ratio ($P_{\gg}/4 e^-$) is two times the ‘P/O’ ratio ($P_{\gg}/2 e^-$) of classical bioenergetics.
 507 P_{\gg}/O_2 is a generalized symbol, not specific for determination of P_i consumption (P_i/O_2 flux
 508 ratio), ADP depletion (ADP/ O_2 flux ratio), or ATP production (ATP/ O_2 flux ratio). The
 509 mechanistic P_{\gg}/O_2 ratio—or P_{\gg}/O_2 stoichiometry—is calculated from the proton-to- O_2 and
 510 proton-to-phosphorylation coupling stoichiometries (**Figure 2B**):
 511

$$512 \quad P_{\gg}/O_2 = \frac{H^+_{pos}/O_2}{H^+_{neg}/P_{\gg}} \quad (1)$$

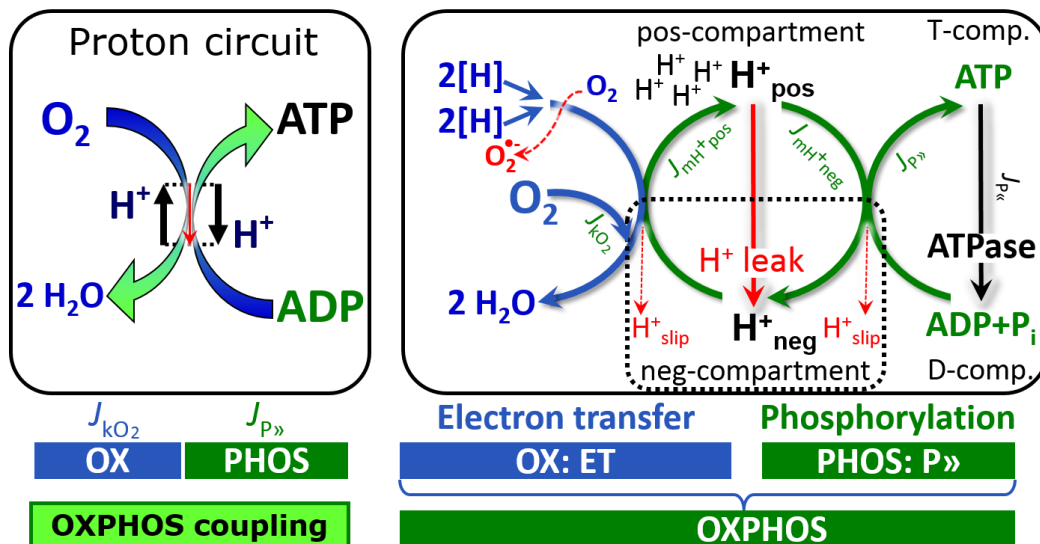
513 The H^+_{pos}/O_2 *coupling stoichiometry* (referring to the full 4 electron reduction of O_2) depends
 514 on the ET-pathway control state, which defines the relative involvement of the three coupling
 515 sites (CI, CIII and CIV) in the catabolic pathway of electrons from the oxidation of reduced
 516 fuel substrates (electron donors) to the reduction of O_2 (electron acceptor). This varies with: (1)
 517 a bypass of CI by single or multiple electron input into the Q-junction; and (2) a bypass of CIV
 518 by involvement of alternative oxidases, AOX, which are not expressed in mammalian
 519 mitochondria.
 520

521 H^+_{pos}/O_2 is 12 in the ET-pathways involving CIII and CIV as proton pumps, increasing to
 522 20 for the NADH-pathway through CI (**Figure 2B**), but a general consensus on H^+_{pos}/O_2
 523 stoichiometries remains to be reached (Hinkle 2005; Wikström and Hummer 2012; Sazanov
 524 2015). The H^+_{neg}/P_{\gg} coupling stoichiometry (3.7; **Figure 2B**) is the sum of $2.7 H^+_{neg}$ required
 525 by the F-ATPase of vertebrate and most invertebrate species (Watt *et al.* 2010) and the proton
 526 balance in the translocation of ADP, ATP and P_i (**Figure 2C**). Taken together, the mechanistic
 527 P_{\gg}/O_2 ratio is calculated at 5.4 and 3.3 for NADH- and succinate-linked respiration, respectively
 528 (Eq. 1). The corresponding classical P_{\gg}/O ratios (referring to the 2 electron reduction of $0.5 O_2$)
 529 are 2.7 and 1.6 (Watt *et al.* 2010), in agreement with the measured P_{\gg}/O ratio for succinate of
 530 1.58 ± 0.02 (Gnaiger *et al.* 2000).
 531

532 The effective P_{\gg}/O_2 flux ratio ($Y_{P_{\gg}/O_2} = J_{P_{\gg}}/J_{kO_2}$; **Figure 3**) is diminished relative to the
 533 mechanistic P_{\gg}/O_2 ratio by intrinsic and extrinsic uncoupling and dyscoupling (**Figure 4**). Such
 534 generalized uncoupling is different from switching to mitochondrial pathways that involve
 535 fewer than three proton pumps (‘coupling sites’: Complexes CI, CIII and CIV), bypassing CI
 536 through multiple electron entries into the Q-junction, or CIII and CIV through AOX (**Figure**
 537 **2B**). Reprogramming of mitochondrial pathways leading to different types of substrates being
 538 oxidized may be considered as a switch of gears (changing the stoichiometry by altering the
 539 substrate that is oxidized) rather than uncoupling (loosening the tightness of coupling relative
 540 to a fixed stoichiometry). In addition, Y_{P_{\gg}/O_2} depends on several experimental conditions of flux
 541 control, increasing as a hyperbolic function of [ADP] to a maximum value (Gnaiger 2001).
 542

543 **Control and regulation:** The terms metabolic *control* and *regulation* are frequently used
 544 synonymously, but are distinguished in metabolic control analysis: ‘We could understand the
 545 regulation as the mechanism that occurs when a system maintains some variable constant over
 546 time, in spite of fluctuations in external conditions (homeostasis of the internal state). On the
 547 other hand, metabolic control is the power to change the state of the metabolism in response to
 548 an external signal’ (Fell 1997). Respiratory control may be induced by experimental control
 549 signals that *exert* an influence on: (1) ATP demand and ADP phosphorylation-rate; (2) fuel
 548 substrate composition, pathway competition; (3) available amounts of substrates and O_2 , *e.g.*,
 549 starvation and hypoxia; (4) the protonmotive force, redox states, flux–force relationships,

550 coupling and efficiency; (5) Ca^{2+} and other ions including H^+ ; (6) inhibitors, *e.g.*, nitric oxide
 551 or intermediary metabolites such as oxaloacetate; (7) signalling pathways and regulatory
 552 proteins, *e.g.*, insulin resistance, transcription factor hypoxia inducible factor 1. *Mechanisms* of
 553 respiratory control and regulation include adjustments of: (1) enzyme activities by allosteric
 554 mechanisms and phosphorylation; (2) enzyme content, concentrations of cofactors and
 555 conserved moieties—such as adenylates, nicotinamide adenine dinucleotide [NAD^+/NADH],
 556 coenzyme Q, cytochrome *c*; (3) metabolic channeling by supercomplexes; and (4)
 557 mitochondrial density (enzyme concentrations and membrane area) and morphology (cristae
 558 folding, fission and fusion). Mitochondria are targeted directly by hormones, thereby affecting
 559 their energy metabolism (Lee *et al.* 2013; Gerö and Szabo 2016; Price and Dai 2016; Moreno
 560 *et al.* 2017). Evolutionary or acquired differences in the genetic and epigenetic basis of
 561 mitochondrial function (or dysfunction) between subjects and gene therapy; age; gender,
 562 biological sex, and hormone concentrations; life style including exercise and nutrition; and
 563 environmental issues including thermal, atmospheric, toxicological and pharmacological
 564 factors, exert an influence on all control mechanisms listed above. For reviews, see Brown
 565 1992; Gnaiger 1993a, 2009; 2014; Paradies *et al.* 2014; Morrow *et al.* 2017.
 566



567 **Figure 3. Coupling in oxidative phosphorylation (OXPHOS)**
 568 $2[\text{H}]$ indicates the reduced hydrogen equivalents of fuel substrates of the catabolic reaction k
 569 with oxygen. O_2 flux, $J_{k\text{O}_2}$, through the catabolic ET-pathway, is coupled to flux through the
 570 phosphorylation-pathway of ADP to ATP, $J_{P\gg}$. The redox proton pumps of the ET-pathway
 571 drive proton flux into the positive (pos) compartment, $J_{m\text{H}^+\text{pos}}$, generating the output
 572 protonmotive force (motive, subscript m). F-ATPase is coupled to inward proton current into
 573 the negative (neg) compartment, $J_{m\text{H}^+\text{neg}}$, to phosphorylate $\text{ADP}+\text{P}_i$ to ATP. The system is
 574 defined by the boundaries (full black line) and is not a black box, but is analysed as a
 575 compartmental system. The negative compartment (neg-compartment, enclosed by the dotted
 576 line) is the matrix space, separated by the mtIM from the positive compartment (pos-
 577 compartment). $\text{ADP}+\text{P}_i$ and ATP are the substrate- and product-compartments (scalar ADP and
 578 ATP compartments, D-comp. and T-comp.), respectively. At steady-state proton turnover,
 579 $J_{\infty\text{H}^+}$, and ATP turnover, $J_{\infty\text{P}}$, maintain concentrations constant, when $J_{m\text{H}^+\infty} = J_{m\text{H}^+\text{pos}} = J_{m\text{H}^+\text{neg}}$,
 580 and $J_{P\infty} = J_{P\gg} = J_{P\ll}$. Modified from Gnaiger (2014).
 581

582 **Respiratory control and response:** Lack of control by a metabolic pathway, *e.g.*,
 583 phosphorylation-pathway, means that there will be no response to a variable activating it, *e.g.*,
 584 $[\text{ADP}]$. The reverse, however, is not true as the absence of a response to $[\text{ADP}]$ does not exclude
 585 the phosphorylation-pathway from having some degree of control. The degree of control of a

586 component of the OXPHOS-pathway on an output variable—such as O₂ flux, will in general
 587 be different from the degree of control on other outputs—such as phosphorylation-flux or
 588 proton leak flux. Therefore, it is necessary to be specific as to which input and output are under
 589 consideration (Fell 1997).

590 **Respiratory coupling control and ET-pathway control:** Respiratory control refers to
 591 the ability of mitochondria to adjust O₂ flux in response to external control signals by engaging
 592 various mechanisms of control and regulation. Respiratory control is monitored in a
 593 mitochondrial preparation under conditions defined as respiratory states. When
 594 phosphorylation of ADP to ATP is stimulated or depressed, an increase or decrease is observed
 595 in electron transfer measured as O₂ flux in respiratory coupling states of intact mitochondria
 596 (‘controlled states’ in the classical terminology of bioenergetics). Alternatively, coupling of
 597 electron transfer with phosphorylation is disengaged by uncouplers. These protonophores are
 598 weak lipid-soluble acids which disrupt the barrier function of the mtIM and thus shortcircuit
 599 the protonmotive system, functioning like a clutch in a mechanical system. The corresponding
 600 coupling control state is characterized by a high O₂ flux without control by P_o (‘uncontrolled
 601 state’).

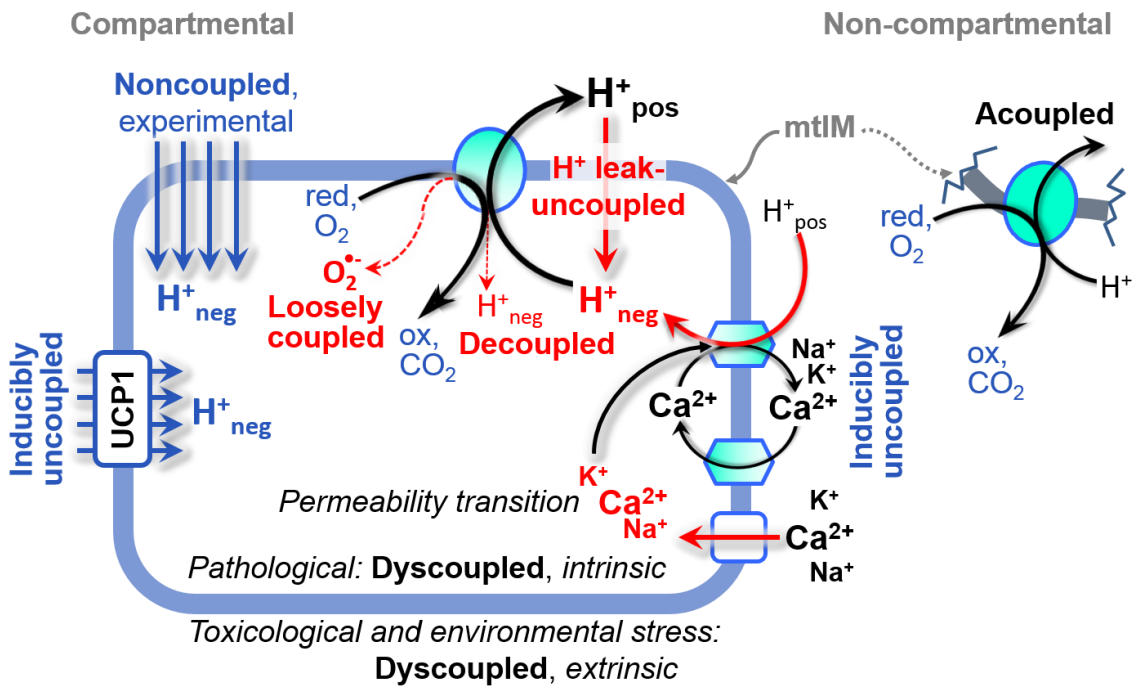
602 ET-pathway control states are obtained in mitochondrial preparations by depletion of
 603 endogenous substrates and addition to the mitochondrial respiration medium of fuel substrates
 604 (2[H] in **Figure 3**) and specific inhibitors, activating selected mitochondrial catabolic pathways,
 605 k, of electron transfer from the oxidation of fuel substrates to reduction of O₂ (**Figure 2A**).
 606 Coupling control states and pathway control states are complementary, since mitochondrial
 607 preparations depend on an exogenous supply of pathway-specific fuel substrates and oxygen
 608 (Gnaiger 2014).

609 **Coupling:** In mitochondrial electron transfer, vectorial transmembrane proton flux is
 610 coupled through the redox proton pumps CI, CIII and CIV to the catabolic flux of scalar
 611 reactions, collectively measured as O₂ flux (**Figure 3**). Thus mitochondria are elements of
 612 energy transformation. Energy is a conserved quantity and cannot be lost or produced in any
 613 internal process (First Law of thermodynamics). Open and closed systems can gain or lose
 614 energy only by external fluxes—by exchange with the environment. Therefore, energy can
 615 neither be produced by mitochondria, nor is there any internal process without energy
 616 conservation. Exergy is defined as the Gibbs energy (‘free energy’) with the potential to
 617 perform work under conditions of constant volume and pressure. *Coupling* is the interaction of
 618 an exergonic process (spontaneous, negative exergy change) with an endergonic process
 619 (positive exergy change) in energy transformations which conserve part of the exergy that
 620 would be irreversibly lost or dissipated in an uncoupled process.

621 **Uncoupling:** Uncoupling of mitochondrial respiration is a general term comprising
 622 diverse mechanisms:

- 623 1. Proton leak across the mtIM from the pos- to the neg-compartment (**Figure 3**);
- 624 2. Cycling of other cations, strongly stimulated by permeability transition, or
 625 experimentally induced by valinomycin in the presence of K⁺;
- 626 3. Proton slip in the redox proton pumps when protons are effectively not pumped (CI,
 627 CIII and CIV) or are not driving phosphorylation (F-ATPase);
- 628 4. Loss of vesicular (compartmental) integrity when electron transfer is acoupled;
- 629 5. Electron leak in the loosely coupled univalent reduction of O₂ to superoxide (O₂^{•-};
 630 superoxide anion radical).

631 Differences of terms—uncoupled vs. noncoupled—are easily overlooked, although they relate
 632 to different meanings of uncoupling (**Figure 4**).



633
634
635
636
637
638
639
640
641
642
643
644
645
646

Figure 4. Mechanisms of respiratory uncoupling

An intact mitochondrial inner membrane, mtIM, is required for vectorial, compartmental coupling. ‘Acoupled’ respiration is the consequence of structural disruption with catalytic activity of non-compartmental mitochondrial fragments. Inducibly uncoupled (activation of UCP1) and experimentally noncoupled respiration (titration of protonophores) stimulate respiration to maximum O₂ flux. H⁺ leak-uncoupled, decoupled, and loosely coupled respiration are components of intrinsic uncoupling. Pathological dysfunction may affect all types of uncoupling, including permeability transition, causing intrinsically dyscoupled respiration. Similarly, toxicological and environmental stress factors can cause extrinsically dyscoupled respiration.

2.2. Coupling states and respiratory rates

Respiratory capacities in coupling control states: To extend the classical nomenclature on mitochondrial coupling states (Section 2.3) by a concept-driven terminology that explicitly incorporates information on the meaning of respiratory states, the terminology must be general and not restricted to any particular experimental protocol or mitochondrial preparation (Gnaiger 2009). Concept-driven nomenclature aims at mapping the *meaning and concept behind* the words and acronyms onto the *forms* of words and acronyms (Miller 1991). The focus of concept-driven nomenclature is primarily the conceptual ‘why’, along with clarification of the experimental ‘how’. Respiratory capacities delineate, comparable to channel capacity in information theory (Schneider 2006), the upper bound of the rate of respiration measured in defined coupling control states and electron transfer-pathway (ET-pathway) states (Figure 5).

To provide a diagnostic reference for respiratory capacities of core energy metabolism, the capacity of *oxidative phosphorylation*, OXPHOS, is measured at kinetically-saturating concentrations of ADP and P_i. The *oxidative ET-capacity* reveals the limitation of OXPHOS-capacity mediated by the *phosphorylation-pathway*. The ET- and phosphorylation-pathways comprise coupled segments of the OXPHOS-system. ET-capacity is measured as noncoupled respiration by application of *external uncouplers*. The contribution of *intrinsically uncoupled* O₂ consumption is studied by preventing the stimulation of phosphorylation either in the absence of ADP or by inhibition of the phosphorylation-pathway. The corresponding states are collectively classified as LEAK-states, when O₂ consumption compensates mainly for ion

665

666 leaks, including the proton leak. Defined coupling states are induced by: (1) adding cation
 667 chelators such as EGTA, binding free Ca^{2+} and thus limiting cation cycling; (2) adding ADP
 668 and P_i ; (3) inhibiting the phosphorylation-pathway; and (4) uncoupler titrations, while
 669 maintaining a defined ET-pathway state with constant fuel substrates and inhibitors of specific
 670 branches of the ET-pathway (**Figure 5**).

671

672 **Figure 5. Four-compartment model of oxidative phosphorylation**

673 Respiratory states (ET, OXPHOS, LEAK; **Table 1**) and corresponding rates (E , P , L) are
 674 connected by the protonmotive force, Δp . ET-capacity, E (I), is
 675 partitioned into (2) dissipative LEAK-respiration, L , when the
 676 Gibbs energy change of catabolic

677 O_2 flux is irreversibly lost, (3) net OXPHOS-capacity, $P-L$, with partial conservation of the
 678 capacity to perform work, and (4) the excess capacity, $E-P$. Modified from Gnaiger (2014).

685

686 **Table 1. Coupling states and residual oxygen consumption in mitochondrial preparations in relation to respiration- and phosphorylation-flux, J_{KO_2} and J_{P} , and protonmotive force, Δp .** Coupling states are established at kinetically-saturating concentrations of fuel substrates and O_2 .

689

State	J_{KO_2}	J_{P}	Δp	Inducing factors	Limiting factors
LEAK	L ; low, cation leak-dependent respiration	0	max.	proton leak, slip, and cation cycling	$J_{\text{P}} = 0$: (1) without ADP, L_N ; (2) max. ATP/ADP ratio, L_T ; or (3) inhibition of the phosphorylation-pathway, L_{Omy}
OXPHOS	P ; high, ADP-stimulated respiration	max.	high	kinetically-saturating [ADP] and [P_i]	J_{P} , by phosphorylation-pathway; or J_{KO_2} by ET-capacity
ET	E ; max., noncoupled respiration	0	low	optimal external uncoupler concentration for max. $J_{\text{O}_2, E}$	J_{KO_2} by ET-capacity
ROX	R_{ox} ; min., residual O_2 consumption	0	0	$J_{\text{O}_2, R_{\text{ox}}}$ in non-ET-pathway oxidation reactions	inhibition of all ET-pathways; or absence of fuel substrates

690

691 The three coupling states, ET, LEAK and OXPHOS, are shown schematically with the
 692 corresponding respiratory rates, abbreviated as E , L and P , respectively (**Figure 5**). We
 693 distinguish metabolic *pathways* from metabolic *states* and the corresponding metabolic *rates*;
 694 for example: ET-pathways (**Figure 5**), ET-states (**Figure 6C**), and ET-capacities, E ,
 695 respectively (**Table 1**). The protonmotive force is *high* in the OXPHOS-state when it drives
 696 phosphorylation, *maximum* in the LEAK-state of coupled mitochondria, driven by LEAK-

697 respiration at a minimum back
698 flux of cations to the matrix
699 side, and *very low* in the ET-
700 state when uncouplers short-
701 circuit the proton cycle (**Table**
702 **1**).

703 **LEAK-state** (**Figure**
704 **6A**): The LEAK-state is defined
705 as a state of mitochondrial
706 respiration when O_2 flux mainly
707 compensates for ion leaks in the
708 absence of ATP synthesis, at
709 kinetically-saturating
710 concentrations of O_2 and
711 respiratory fuel substrates.
712 LEAK-respiration is measured
713 to obtain an estimate of *intrinsic*
714 *uncoupling* without addition of
715 an experimental uncoupler: (1)
716 in the absence of adenylates,
717 *i.e.*, AMP, ADP and ATP; (2)
718 after depletion of ADP at a
719 maximum ATP/ADP ratio; or
720 (3) after inhibition of the
721 phosphorylation-pathway by
722 inhibitors of F-ATPase—such
723 as oligomycin, or of adenine
724 nucleotide translocase—such as
725 carboxyatractyloside.

726 Adjustment of the nominal
727 concentration of these inhibitors
728 to the density of biological
729 sample applied can minimize or
730 avoid inhibitory side-effects
731 exerted on ET-capacity or even
732 some dyscoupling.

733 **Proton leak and**
734 **uncoupled respiration:** Proton
735 leak is a leak current of protons.
736 The intrinsic proton leak is the
737 *uncoupled* process in which
738 protons diffuse across the mtIM
739 in the dissipative direction of the
740 downhill protonmotive force

741 without coupling to phosphorylation (**Figure 6A**). The proton leak flux depends non-linearly
742 on the protonmotive force (Garlid *et al.* 1989; Divakaruni and Brand 2011), it is a property of
743 the mtIM and may be enhanced due to possible contaminations by free fatty acids. Inducible
744 uncoupling mediated by uncoupling protein 1 (UCP1) is physiologically controlled, *e.g.*, in
745 brown adipose tissue. UCP1 is a member of the mitochondrial carrier family which is involved
746 in the translocation of protons across the mtIM (Klingenberg 2017). Consequently, the short-

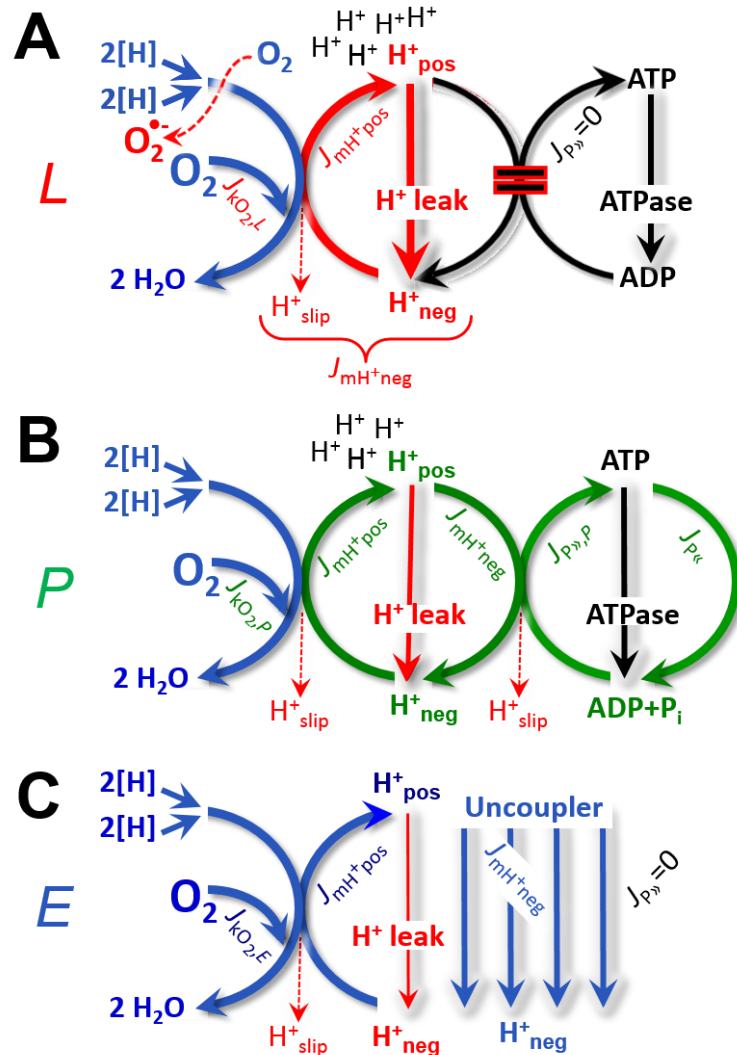


Figure 6. Respiratory coupling states

(A) **LEAK-state and rate, *L***: Phosphorylation is arrested, $J_{P_{\gg}} = 0$, and catabolic O_2 flux, $J_{kO_2,L}$, is controlled mainly by the proton leak, $J_{mH^{+neg,L}}$, at maximum protonmotive force (**Figure 4**).

(B) **OXPHOS-state and rate, *P***: Phosphorylation, $J_{P_{\gg}}$, is stimulated by kinetically-saturating [ADP] and [P₁], and is supported by a high protonmotive force. O_2 flux, $J_{kO_2,P}$, is well-coupled at a P_{\gg}/O_2 ratio of $J_{P_{\gg},P}/J_{O_2,P}$.

(C) **ET-state and rate, *E***: Noncoupled respiration, $J_{kO_2,E}$, is maximum at optimum exogenous uncoupler concentration and phosphorylation is zero, $J_{P_{\gg}} = 0$. See also **Figure 3**.

747 circuit diminishes the protonmotive force and stimulates electron transfer to O₂ and heat
748 dissipation without phosphorylation of ADP.

749 **Cation cycling:** There can be other cation contributors to leak current including calcium
750 and probably magnesium. Calcium current is balanced by mitochondrial Na⁺/Ca²⁺ exchange,
751 which is balanced by Na⁺/H⁺ or K⁺/H⁺ exchanges. This is another effective uncoupling
752 mechanism different from proton leak (**Table 2**).

753

754 **Table 2. Terms on respiratory coupling and uncoupling.**

Term	J_{kO_2}	$P \gg O_2$	Note	
acoupled		0	electron transfer in mitochondrial fragments without vectorial proton translocation (Figure 4)	
intrinsic, no protonophore added	uncoupled	L	0	non-phosphorylating LEAK-respiration (Figure 6A)
	proton leak-uncoupled		0	component of L , H ⁺ diffusion across the mtIM (Figure 4)
	decoupled		0	component of L , proton slip (Figure 4)
	loosely coupled		0	component of L , lower coupling due to superoxide formation and bypass of proton pumps (Figure 4)
	dyscoupled		0	pathologically, toxicologically, environmentally increased uncoupling, mitochondrial dysfunction
	inducibly uncoupled		0	by UCP1 or cation (<i>e.g.</i> , Ca ²⁺) cycling (Figure 4)
noncoupled	E	0	non-phosphorylating respiration stimulated to maximum flux at optimum exogenous uncoupler concentration (Figure 6C)	
well-coupled	P	high	phosphorylating respiration with an intrinsic LEAK component (Figure 6B)	
fully coupled	$P - L$	max.	OXPPOS-capacity corrected for LEAK-respiration (Figure 5)	

755

756 **Proton slip and decoupled respiration:** Proton slip is the *decoupled* process in which
757 protons are only partially translocated by a redox proton pump of the ET-pathways and slip
758 back to the original vesicular compartment. The proton leak is the dominant contributor to the
759 overall leak current in mammalian mitochondria incubated under physiological conditions at
760 37 °C, whereas proton slip is increased at lower experimental temperature (Canton *et al.* 1995).
761 Proton slip can also happen in association with the F-ATPase, in which the proton slips downhill
762 across the pump to the matrix without contributing to ATP synthesis. In each case, proton slip
763 is a property of the proton pump and increases with the pump turnover rate.

764 **Electron leak and loosely coupled respiration:** Superoxide production by the ETS leads
765 to a bypass of redox proton pumps and correspondingly lower $P \gg O_2$ ratio. This depends on the
766 actual site of electron leak and the scavenging of hydrogen peroxide by cytochrome *c*, whereby
767 electrons may re-enter the ETS with proton translocation by CIV.

768 **Loss of compartmental integrity and acoupled respiration:** Electron transfer and
769 catabolic O₂ flux proceed without compartmental proton translocation in disrupted
770 mitochondrial fragments. Such fragments form during mitochondrial isolation, and may not
771 fully fuse to re-establish structurally intact mitochondria. Loss of mtIM integrity, therefore, is

772 the cause of acoupled respiration, which is a nonvectorial dissipative process without control
773 by the protonmotive force.

774 **Dyscoupled respiration:** Mitochondrial injuries may lead to *dyscoupling* as a
775 pathological or toxicological cause of *uncoupled* respiration. Dyscoupling may involve any
776 type of uncoupling mechanism, *e.g.*, opening the permeability transition pore. Dyscoupled
777 respiration is distinguished from the experimentally induced *noncoupled* respiration in the ET-
778 state (**Table 2**).

779 **OXPHOS-state (Figure 6B):** The OXPHOS-state is defined as the respiratory state with
780 kinetically-saturating concentrations of O₂, respiratory and phosphorylation substrates, and
781 absence of exogenous uncoupler, which provides an estimate of the maximal respiratory
782 capacity in the OXPHOS-state for any given ET-pathway state. Respiratory capacities at
783 kinetically-saturating substrate concentrations provide reference values or upper limits of
784 performance, aiming at the generation of data sets for comparative purposes. Physiological
785 activities and effects of substrate kinetics can be evaluated relative to the OXPHOS-capacity.

786 As discussed previously, 0.2 mM ADP does not fully saturate flux in isolated
787 mitochondria (Gnaiger 2001; Puchowicz *et al.* 2004); greater ADP concentration is required,
788 particularly in permeabilized muscle fibres and cardiomyocytes, to overcome limitations by
789 intracellular diffusion and by the reduced conductance of the mtOM (Jepihhina *et al.* 2011,
790 Illaste *et al.* 2012, Simson *et al.* 2016), either through interaction with tubulin (Rostovtseva *et al.*
791 2008) or other intracellular structures (Birkedal *et al.* 2014). In permeabilized muscle fibre
792 bundles of high respiratory capacity, the apparent K_m for ADP increases up to 0.5 mM (Saks *et al.*
793 1998), consistent with experimental evidence that >90% saturation is reached only at >5
794 mM ADP (Pesta and Gnaiger 2012). Similar ADP concentrations are also required for accurate
795 determination of OXPHOS-capacity in human clinical cancer samples and permeabilized cells
796 (Klepinin *et al.* 2016; Koit *et al.* 2017). Whereas 2.5 to 5 mM ADP is sufficient to obtain the
797 actual OXPHOS-capacity in many types of permeabilized tissue and cell preparations,
798 experimental validation is required in each specific case.

799 **Electron transfer-state (Figure 6C):** The ET-state is defined as the *noncoupled* state
800 with kinetically-saturating concentrations of O₂, respiratory substrate and optimum *exogenous*
801 uncoupler concentration for maximum O₂ flux. O₂ flux determined in the ET-state yields an
802 estimate of ET-capacity. Inhibition of respiration is observed above optimum uncoupler
803 concentrations. As a consequence of the nearly collapsed protonmotive force, the driving force
804 is insufficient for phosphorylation, and $J_{P_{\gg}} = 0$.

805 **ROX state and Rox:** Besides the three fundamental coupling states of mitochondrial
806 preparations, the state of residual O₂ consumption, ROX, is relevant to assess respiratory
807 function (**Figure 1**). ROX is not a coupling state. The rate of residual oxygen consumption,
808 *Rox*, is defined as O₂ consumption due to oxidative reactions measured after inhibition of ET—
809 with rotenone, malonic acid and antimycin A. Cyanide and azide inhibit not only CIV but
810 catalase and several peroxidases involved in *Rox*. However, high concentrations of antimycin
811 A, but not rotenone or cyanide, inhibit peroxisomal acyl-CoA oxidase and D-amino acid
812 oxidase (Vamecq *et al.* 1987). ROX represents a baseline that is used to correct respiration
813 measured in defined coupling states. *Rox*-corrected *L*, *P* and *E* not only lower the values of total
814 fluxes, but also changes the flux control ratios *L/P* and *L/E*. *Rox* is not necessarily equivalent
815 to non-mitochondrial reduction of O₂, considering O₂-consuming reactions in mitochondria that
816 are not related to ET—such as O₂ consumption in reactions catalyzed by monoamine oxidases
817 (type A and B), monooxygenases (cytochrome P450 monooxygenases), dioxygenase (sulfur
818 dioxygenase and trimethyllysine dioxygenase), and several hydroxylases. Even isolated
819 mitochondrial fractions, especially those obtained from liver, may be contaminated by
820 peroxisomes. This fact makes the exact determination of mitochondrial O₂ consumption and
821 mitochondria-associated generation of reactive oxygen species complicated (Schönfeld *et al.*
822 2009; Speijer 2016; **Figure 2**). The dependence of ROX-linked O₂ consumption needs to be

823 studied in detail together with non-ET enzyme activities, availability of specific substrates, O₂
824 concentration, and electron leakage leading to the formation of reactive oxygen species.

825 **Quantitative relations:** E may exceed or be equal to P . $E > P$ is observed in many types
826 of mitochondria, varying between species, tissues and cell types (Gnaiger 2009). $E - P$ is the
827 excess ET-capacity pushing the phosphorylation-flux (**Figure 2C**) to the limit of its *capacity of*
828 *utilizing* the protonmotive force. In addition, the magnitude of $E - P$ depends on the tightness of
829 respiratory coupling or degree of uncoupling, since an increase of L causes P to increase
830 towards the limit of E . The *excess* $E - P$ capacity, $E - P$, therefore, provides a sensitive diagnostic
831 indicator of specific injuries of the phosphorylation-pathway, under conditions when E remains
832 constant but P declines relative to controls (**Figure 5**). Substrate cocktails supporting
833 simultaneous convergent electron transfer to the Q-junction for reconstitution of TCA cycle
834 function establish pathway control states with high ET-capacity, and consequently increase the
835 sensitivity of the $E - P$ assay.

836 E cannot theoretically be lower than P . $E < P$ must be discounted as an artefact, which
837 may be caused experimentally by: (1) loss of oxidative capacity during the time course of the
838 respirometric assay, since E is measured subsequently to P ; (2) using insufficient uncoupler
839 concentrations; (3) using high uncoupler concentrations which inhibit ET (Gnaiger 2008); (4)
840 high oligomycin concentrations applied for measurement of L before titrations of uncoupler,
841 when oligomycin exerts an inhibitory effect on E . On the other hand, the excess ET-capacity is
842 overestimated if non-saturating [ADP] or [P_i] are used. See State 3 in the next section.

843 The net OXPHOS-capacity is calculated by subtracting L from P (**Figure 5**). The net
844 $P \gg O_2$ equals $P \gg (P - L)$, wherein the dissipative LEAK component in the OXPHOS-state may
845 be overestimated. This can be avoided by measuring LEAK-respiration in a state when the
846 protonmotive force is adjusted to its slightly lower value in the OXPHOS-state—by titration of
847 an ET inhibitor (Divakaruni and Brand 2011). Any turnover-dependent components of proton
848 leak and slip, however, are underestimated under these conditions (Garlid *et al.* 1993). In
849 general, it is inappropriate to use the term *ATP production* or *ATP turnover* for the difference
850 of O₂ flux measured in the OXPHOS and LEAK states. $P - L$ is the upper limit of OXPHOS-
851 capacity that is freely available for ATP production (corrected for LEAK-respiration) and is
852 fully coupled to phosphorylation with a maximum mechanistic stoichiometry (**Figure 5**).

853 The rates of LEAK respiration and OXPHOS capacity depend on (1) the tightness of
854 coupling under the influence of the respiratory uncoupling mechanisms (**Figure 4**), and (2) the
855 coupling stoichiometry which varies as a function of the substrate type undergoing oxidation in
856 ET-pathways with either two or three coupling sites (**Figure 2B**). When cocktails with NADH-
857 linked substrates and succinate are used, the relative contribution of ET-pathways with three or
858 two coupling sites cannot be controlled experimentally, is difficult to determine, and may shift
859 in transitions between LEAK-, OXPHOS- and ET-states (Gnaiger 2014). Under these
860 experimental conditions, we cannot separate the tightness of coupling *versus* coupling
861 stoichiometry as the mechanisms of respiratory control in the shift of L/P ratios. The tightness
862 of coupling and fully coupled O₂ flux, $P - L$ (**Table 2**), therefore, are obtained from
863 measurements of coupling control of LEAK respiration, OXPHOS- and ET-capacities in well
864 defined pathway states, using either pyruvate and malate as substrates or the classical succinate
865 and rotenone substrate-inhibitor combination (**Figure 2B**).

866 2.3. Classical terminology for isolated mitochondria

867 *'When a code is familiar enough, it ceases appearing like a code; one forgets that there*
868 *is a decoding mechanism. The message is identical with its meaning'* (Hofstadter 1979).

870

871 Chance and Williams (1955; 1956) introduced five classical states of mitochondrial
872 respiration and cytochrome redox states. **Table 3** shows a protocol with isolated mitochondria

873 in a closed respirometric chamber, defining a sequence of respiratory states. States and rates
874 are not specifically distinguished in this nomenclature.

875

876

877

878

Table 3. Metabolic states of mitochondria (Chance and Williams, 1956; Table V).

State	[O ₂]	ADP level	Substrate level	Respiration rate	Rate-limiting substance
1	>0	low	low	slow	ADP
2	>0	high	~0	slow	substrate
3	>0	high	high	fast	respiratory chain
4	>0	low	high	slow	ADP
5	0	high	high	0	oxygen

879

880

881

882

State 1 is obtained after addition of isolated mitochondria to air-saturated isoosmotic/isotonic respiration medium containing P_i, but no fuel substrates and no adenylates, *i.e.*, AMP, ADP, ATP.

883

884

885

886

887

888

889

890

891

892

893

894

State 2 is induced by addition of a ‘high’ concentration of ADP (typically 100 to 300 μM), which stimulates respiration transiently on the basis of endogenous fuel substrates and phosphorylates only a small portion of the added ADP. State 2 is then obtained at a low respiratory activity limited by exhausted endogenous fuel substrate availability (**Table 3**). If addition of specific inhibitors of respiratory complexes—such as rotenone—does not cause a further decline of O₂ flux, State 2 is equivalent to the ROX state (See below.). If inhibition is observed, undefined endogenous fuel substrates are a confounding factor of pathway control, contributing to the effect of subsequently externally added substrates and inhibitors. In contrast to the original protocol, an alternative sequence of titration steps is frequently applied, in which the alternative ‘State 2’ has an entirely different meaning, when this second state is induced by addition of fuel substrate without ADP (LEAK-state; in contrast to State 2 defined in **Table 1** as a ROX state), followed by addition of ADP.

895

896

897

898

899

900

901

902

903

904

905

906

907

State 3 is the state stimulated by addition of fuel substrates while the ADP concentration is still high (**Table 3**) and supports coupled energy transformation through oxidative phosphorylation. ‘High ADP’ is a concentration of ADP specifically selected to allow the measurement of State 3 to State 4 transitions of isolated mitochondria in a closed respirometric chamber. Repeated ADP titration re-establishes State 3 at ‘high ADP’. Starting at O₂ concentrations near air-saturation (ca. 200 μM O₂ at sea level and 37 °C), the total ADP concentration added must be low enough (typically 100 to 300 μM) to allow phosphorylation to ATP at a coupled O₂ flux that does not lead to O₂ depletion during the transition to State 4. In contrast, kinetically-saturating ADP concentrations usually are 10-fold higher than ‘high ADP’, *e.g.*, 2.5 mM in isolated mitochondria. The abbreviation State 3u is occasionally used in bioenergetics, to indicate the state of respiration after titration of an uncoupler, without sufficient emphasis on the fundamental difference between OXPHOS-capacity (*well-coupled* with an *endogenous* uncoupled component) and ET-capacity (*noncoupled*).

908

909

910

911

912

913

914

915

916

State 4 is a LEAK-state that is obtained only if the mitochondrial preparation is intact and well-coupled. Depletion of ADP by phosphorylation to ATP causes a decline of O₂ flux in the transition from State 3 to State 4. Under the conditions of State 4, a maximum protonmotive force and high ATP/ADP ratio are maintained. The gradual decline of Y_{P»/O₂} towards diminishing [ADP] at State 4 must be taken into account for calculation of P»/O₂ ratios (Gnaiger 2001). State 4 respiration, L_T (**Table 1**), reflects intrinsic proton leak and ATP hydrolysis activity. O₂ flux in State 4 is an overestimation of LEAK-respiration if the contaminating ATP hydrolysis activity recycles some ATP to ADP, J_{P«}, which stimulates respiration coupled to phosphorylation, J_{P»} > 0. This can be tested by inhibition of the phosphorylation-pathway using

917 oligomycin, ensuring that $J_{P_s} = 0$ (State 4o). Alternatively, sequential ADP titrations re-
 918 establish State 3, followed by State 3 to State 4 transitions while sufficient O_2 is available.
 919 Anoxia may be reached, however, before exhaustion of ADP (State 5).

920 **State 5** is the state after exhaustion of O_2 in a closed respirometric chamber. Diffusion of
 921 O_2 from the surroundings into the aqueous solution may be a confounding factor preventing
 922 complete anoxia (Gnaiger 2001). Chance and Williams (1955) provide an alternative definition
 923 of State 5, which gives it the different meaning of ROX versus anoxia: ‘State 5 may be obtained
 924 by antimycin A treatment or by anaerobiosis’.

925 In **Table 3**, only States 3 and 4 (and ‘State 2’ in the alternative protocol: addition of fuel
 926 substrates without ADP; not included in the table) are coupling control states, with the
 927 restriction that O_2 flux in State 3 may be limited kinetically by non-saturating ADP
 928 concentrations (**Table 1**).

929
 930

931 3. Normalization: fluxes and flows

932

933 3.1. Normalization: system or sample

934

935 The term *rate* is not sufficiently defined to be useful for reporting data (**Figure 7**). The
 936 inconsistency of the meanings of rate becomes fully apparent when considering Galileo
 937 Galilei’s famous principle, that ‘bodies of different weight all fall at the same rate (have a
 938 constant acceleration)’ (Coopersmith 2010).

939 **Flow per system, I** : In a generalization of electrical terms, flow as an extensive quantity
 940 (I ; per system) is distinguished from flux as a size-specific quantity (J ; per system size) (**Figure**
 941 **7A**). Electric current is flow, I_{el} [$A \equiv C \cdot s^{-1}$] per system (extensive quantity). When dividing this
 942 extensive quantity by system size (cross-sectional area of a ‘wire’), a size-specific quantity is
 943 obtained, which is flux (current density), J_{el} [$A \cdot m^{-2} = C \cdot s^{-1} \cdot m^{-2}$] (**Box 2**).

944

945 **Box 2: Metabolic fluxes and flows: vectorial and scalar**

946

947 Fluxes are *vectors*, if they have *spatial* geometric direction in addition to magnitude.
 948 Electric charge per unit time is electric flow or current, $I_{el} = dQ_{el} \cdot dt^{-1}$ [A]. When expressed per
 949 unit cross-sectional area, A [m^2], a vector flux is obtained, which is current density (surface-
 950 density of flow) perpendicular to the direction of flux, $J_{el} = I_{el} \cdot A^{-1}$ [$A \cdot m^{-2}$] (Cohen et al. 2008).
 951 For all transformations *flows*, I_{tr} , are defined as extensive quantities. Vector and scalar *fluxes*
 952 are obtained as $J_{tr} = I_{tr} \cdot A^{-1}$ [$mol \cdot s^{-1} \cdot m^{-2}$] and $J_{tr} = I_{tr} \cdot V^{-1}$ [$mol \cdot s^{-1} \cdot m^{-3}$], expressing flux as an area-
 953 specific vector or volume-specific vectorial or scalar quantity, respectively (Gnaiger 1993b).
 954 We use the metre–kilogram–second–ampere (MKSA) international system of units (*SI*) for
 955 general cases ([m], [kg], [s] and [A]), with decimal *SI* prefixes for specific applications (**Table**
 956 **4**).

957 We suggest to define: (1) *vectorial* fluxes, which are translocations as functions of
 958 *gradients* with direction in geometric space in continuous systems; (2) *vectorial* fluxes, which
 959 describe translocations in discontinuous systems and are restricted to information on
 960 *compartmental differences* (**Figure 3**, transmembrane proton flux); and (3) *scalar* fluxes, which
 961 are transformations in a *homogenous* system (**Figure 3**, catabolic O_2 flux, J_{KO_2}).

962 Vectorial transmembrane proton fluxes, J_{mH+pos} and J_{mH+neg} , are analyzed in a
 963 heterogenous compartmental system as a quantity with *directional* but not *spatial* information.
 964 Translocation of protons across the mtIM has a defined direction, either from the negative
 965 compartment (matrix space; negative, neg–compartment) to the positive compartment (inter-
 966 membrane space; positive, pos–compartment) or *vice versa* (**Figure 3**). The arrows defining
 967 the direction of the translocation between the two vesicular compartments may point upwards

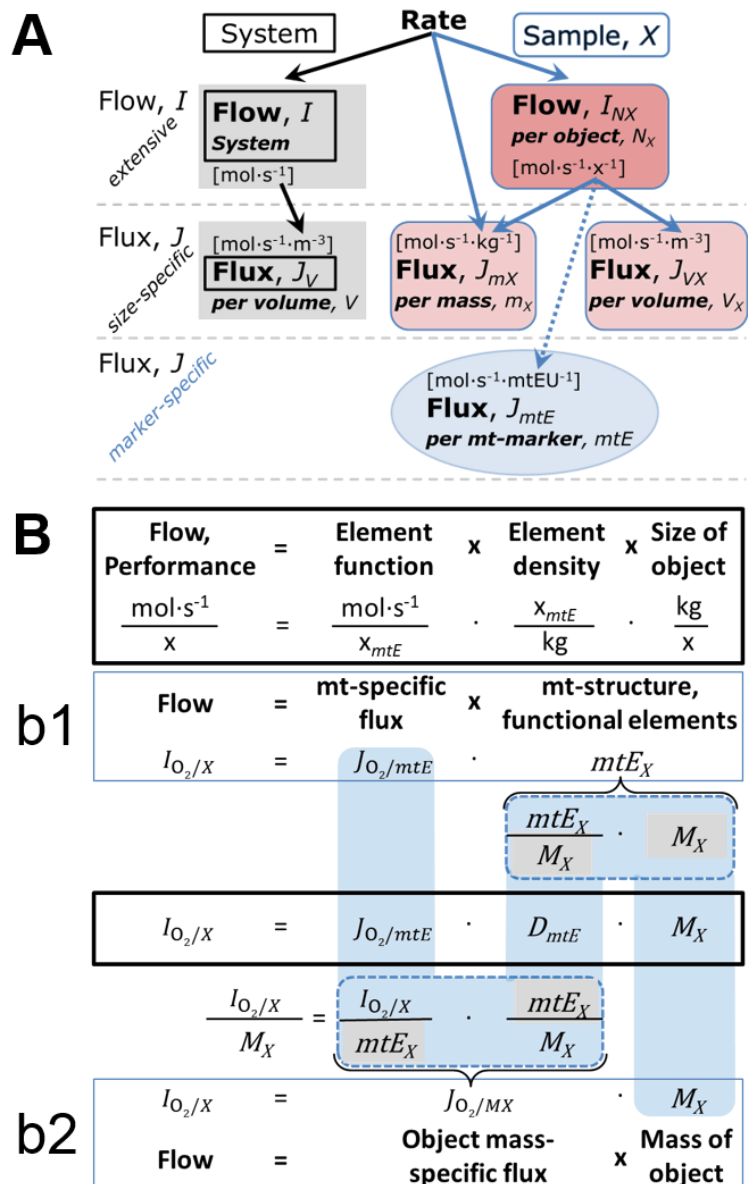
968 or downwards, right or left, without any implication that these are actual directions in space.
 969 The pos-compartment is neither above nor below the neg-compartment in a spatial sense, but
 970 can be visualized arbitrarily in a figure in the upper position (**Figure 3**). In general, the
 971 *compartmental direction* of vectorial translocation from the neg-compartment to the pos-
 972 compartment is defined by assigning the initial and final state as *ergodynamic compartments*,
 973 $H^+_{neg} \rightarrow H^+_{pos}$ or $0 = -1 H^+_{neg} + 1 H^+_{pos}$, related to work (erg = work) that must be performed to
 974 lift the proton from a lower to a higher electrochemical potential or from the lower to the higher
 975 ergodynamic compartment (Gnaiger 1993b).

976 In analogy to *vectorial* translocation, the direction of a *scalar* chemical reaction, $A \rightarrow B$
 977 or $0 = -1 A + 1 B$, is defined by assigning substrates and products, A and B, as ergodynamic
 978 compartments. O_2 is defined as a substrate in respiratory O_2 consumption (electron acceptor),
 979 which together with the fuel substrates (electron donors) comprises the substrate compartment
 980 of the catabolic reaction. Volume-specific scalar O_2 flux is coupled to vectorial translocation,
 981 yielding the H^+_{pos}/O_2 ratio (**Figure 2B**).

982 **Figure 7. Flow and flux, and normalization in structure-function analysis**

983 **(A)** Different meanings of rate may lead to confusion, if the
 984 normalization is not sufficiently specified. Results are frequently
 985 expressed as mass-specific *flux*,
 986 J_{mX} , per mg protein, dry or wet
 987 weight (mass). Cell volume, V_{cell} ,
 988 may be used for normalization
 989 (volume-specific flux, J_{Vcell}),
 990 which must be clearly
 991 distinguished from flow per cell,
 992 I_{Ncell} , or flux, J_V , expressed for
 993 methodological reasons per
 994 volume of the measurement
 995 system.

996 **(B)** O_2 flow, $I_{O_2/X}$, is the product
 997 of performance per functional
 998 element (element function,
 999 mitochondria-specific flux),
 1000 element density (mitochondrial
 1001 density, D_{mtE}), and size of entity X
 1002 (mass, M_X). **(b1)** Structured
 1003 analysis: performance is the
 1004 product of mitochondrial *function*
 1005 (mt-specific flux) and *structure*
 1006 (functional elements; D_{mtE} times
 1007 mass of X). **(b2)** Unstructured
 1008 analysis: performance is the
 1009 product of *entity mass-specific*
 1010 flux, $J_{O_2/MX} = I_{O_2/X}/M_X = I_{O_2}/m_X$
 1011 [$\text{mol}\cdot\text{s}^{-1}\cdot\text{kg}^{-1}$] and *size of entity*,
 1012 expressed as mass of X; $M_X = m_X \cdot N_X^{-1}$ [$\text{kg}\cdot\text{x}^{-1}$]. Modified from
 1013 Gnaiger (2014). For further details see **Table 4**.



1019 **Extensive quantities:** An extensive quantity increases proportionally with system size.
 1020 The magnitude of an extensive quantity is completely additive for non-interacting
 1021 subsystems—such as mass or flow expressed per defined system. The magnitude of these
 1022 quantities depends on the extent or size of the system (Cohen *et al.* 2008).

1023 **Size-specific quantities:** ‘The adjective *specific* before the name of an extensive quantity
 1024 is often used to mean *divided by mass*’ (Cohen *et al.* 2008). In this system-paradigm, mass-
 1025 specific flux is flow divided by mass of the *system* (the total mass of everything within the
 1026 measuring chamber or reactor). A mass-specific quantity is independent of the extent of non-
 1027 interacting homogenous subsystems. Tissue-specific quantities (related to the *sample* in
 1028 contrast to the *system*) are of fundamental interest in the field of comparative mitochondrial
 1029 physiology, where *specific* refers to the *type of the sample* rather than *mass of the system*. The
 1030 term *specific*, therefore, must be clarified; *sample-specific*, *e.g.*, muscle mass-specific
 1031 normalization, is distinguished from *system-specific* quantities (mass or volume; **Figure 7**).

1032

1033 3.2. Normalization for system-size: flux per chamber volume

1034

1035 **System-specific flux, J_{V,O_2} :** The experimental system (experimental chamber) is part of
 1036 the measurement apparatus, separated from the environment as an isolated, closed, open,
 1037 isothermal or non-isothermal system (**Table 4**). On another level, we distinguish between (1)
 1038 the *system* with volume V and mass m defined by the system boundaries, and (2) the *sample* or
 1039 *objects* with volume V_X and mass m_X that are enclosed in the experimental chamber (**Figure 7**).
 1040 Metabolic O_2 flow per object, $I_{O_2/X}$, increases as the mass of the object is increased. Sample
 1041 mass-specific O_2 flux, $J_{O_2/mX}$ should be independent of the mass of the sample studied in the
 1042 instrument chamber, but system volume-specific O_2 flux, J_{V,O_2} (per volume of the instrument
 1043 chamber), should increase in direct proportion to the mass of the sample in the chamber.
 1044 Whereas J_{V,O_2} depends on mass-concentration of the sample in the chamber, it should be
 1045 independent of the chamber (system) volume at constant sample mass. There are practical
 1046 limitations to increase the mass-concentration of the sample in the chamber, when one is
 1047 concerned about crowding effects and instrumental time resolution.

1048 When the reactor volume does not change during the reaction, which is typical for liquid
 1049 phase reactions, the volume-specific flux of a chemical reaction r is the time derivative of the
 1050 advancement of the reaction per unit volume, $J_{V,rB} = d_{r\zeta_B}/dt \cdot V^{-1}$ [(mol·s⁻¹)·L⁻¹]. The rate of
 1051 concentration change is dc_B/dt [(mol·L⁻¹)·s⁻¹], where concentration is $c_B = n_B/V$. There is a
 1052 difference between (1) J_{V,rO_2} [mol·s⁻¹·L⁻¹] and (2) rate of concentration change [mol·L⁻¹·s⁻¹].
 1053 These merge to a single expression only in closed systems. In open systems, external fluxes
 1054 (such as O_2 supply) are distinguished from internal transformations (catabolic flux, O_2
 1055 consumption). In a closed system, external flows of all substances are zero and O_2 consumption
 1056 (internal flow of catabolic reactions k), I_{kO_2} [pmol·s⁻¹], causes a decline of the amount of O_2 in
 1057 the system, n_{O_2} [nmol]. Normalization of these quantities for the volume of the system, V [L \equiv
 1058 dm³], yields volume-specific O_2 flux, $J_{V,kO_2} = I_{kO_2}/V$ [nmol·s⁻¹·L⁻¹], and O_2 concentration, $[O_2]$
 1059 or $c_{O_2} = n_{O_2}/V$ [μ mol·L⁻¹ = μ M = nmol·mL⁻¹]. Instrumental background O_2 flux is due to external
 1060 flux into a non-ideal closed respirometer; then total volume-specific flux has to be corrected for
 1061 instrumental background O_2 flux— O_2 diffusion into or out of the instrumental chamber. J_{V,kO_2}
 1062 is relevant mainly for methodological reasons and should be compared with the accuracy of
 1063 instrumental resolution of background-corrected flux, *e.g.*, ± 1 nmol·s⁻¹·L⁻¹ (Gnaiger 2001).
 1064 ‘Metabolic’ or catabolic indicates O_2 flux, J_{kO_2} , corrected for: (1) instrumental background O_2
 1065 flux; (2) chemical background O_2 flux due to autoxidation of chemical components added to
 1066 the incubation medium; and (3) *Rox* for O_2 -consuming side reactions unrelated to the catabolic
 1067 pathway k .

1068

1069

1070 3.3. Normalization: per sample

1071
1072 The challenges of measuring mitochondrial respiratory flux are matched by those of
1073 normalization. Application of common and defined units is required for direct transfer of
1074 reported results into a database. The second [s] is the *SI* unit for the base quantity *time*. It is also
1075 the standard time-unit used in solution chemical kinetics. A rate may be considered as the
1076 numerator and normalization as the complementary denominator, which are tightly linked in
1077 reporting the measurements in a format commensurate with the requirements of a database.
1078 Normalization (**Table 4**) is guided by physicochemical principles, methodological
1079 considerations, and conceptual strategies (**Figure 7**).

1080
1081 **Table 4. Sample concentrations and normalization of flux.**
1082

Expression	Symbol	Definition	Unit	Notes
Sample				
identity of sample	X	object: cell, tissue, animal, patient		
number of sample entities X	N_X	number of objects	x	
mass of sample X	m_X		kg	1
mass of object X	M_X	$M_X = m_X \cdot N_X^{-1}$	$\text{kg} \cdot \text{x}^{-1}$	1
Mitochondria				
mitochondria	mt	$X = \text{mt}$		
amount of mt-elements	mtE	quantity of mt-marker	mtEU	
Concentrations				
object number concentration	C_{NX}	$C_{NX} = N_X \cdot V^{-1}$	$\text{x} \cdot \text{m}^{-3}$	2
sample mass concentration	C_{mX}	$C_{mX} = m_X \cdot V^{-1}$	$\text{kg} \cdot \text{m}^{-3}$	
mitochondrial concentration	C_{mtE}	$C_{mtE} = mtE \cdot V^{-1}$	$\text{mtEU} \cdot \text{m}^{-3}$	3
specific mitochondrial density	D_{mtE}	$D_{mtE} = mtE \cdot m_X^{-1}$	$\text{mtEU} \cdot \text{kg}^{-1}$	4
mitochondrial content, mtE per object X	mtE_X	$mtE_X = mtE \cdot N_X^{-1}$	$\text{mtEU} \cdot \text{x}^{-1}$	5
O₂ flow and flux				
flow, system	I_{O_2}	internal flow	$\text{mol} \cdot \text{s}^{-1}$	6 7
volume-specific flux	J_{V,O_2}	$J_{V,O_2} = I_{O_2} \cdot V^{-1}$	$\text{mol} \cdot \text{s}^{-1} \cdot \text{m}^{-3}$	8
flow per object X	$I_{O_2/X}$	$I_{O_2/X} = J_{V,O_2} \cdot C_{NX}^{-1}$	$\text{mol} \cdot \text{s}^{-1} \cdot \text{x}^{-1}$	9
mass-specific flux	$J_{O_2/mX}$	$J_{O_2/mX} = J_{V,O_2} \cdot C_{mX}^{-1}$	$\text{mol} \cdot \text{s}^{-1} \cdot \text{kg}^{-1}$	
mitochondria-specific flux	$J_{O_2/mtE}$	$J_{O_2/mtE} = J_{V,O_2} \cdot C_{mtE}^{-1}$	$\text{mol} \cdot \text{s}^{-1} \cdot \text{mtEU}^{-1}$	10

- 1083 1 Units are given in the MKSA system (**Box 2**). The *SI* prefix k is used for the *SI* base unit of mass (kg
1084 = 1,000 g). In praxis, various *SI* prefixes are used for convenience, to make numbers easily readable,
1085 e.g., 1 mg tissue, cell or mitochondrial mass instead of 0.000001 kg.
1086 2 In case sample X = cells, the object number concentration is $C_{N_{\text{cell}}} = N_{\text{cell}} \cdot V^{-1}$, and volume may be
1087 expressed in [$\text{dm}^3 \equiv \text{L}$] or [$\text{cm}^3 = \text{mL}$]. See **Table 5** for different object types.
1088 3 mt-concentration is an experimental variable, dependent on sample concentration: (1) $C_{mtE} = mtE \cdot V^{-1}$;
1089 (2) $C_{mtE} = mtE_X \cdot C_{NX}$; (3) $C_{mtE} = C_{mX} \cdot D_{mtE}$.
1090 4 If the amount of mitochondria, mtE , is expressed as mitochondrial mass, then D_{mtE} is the mass
1091 fraction of mitochondria in the sample. If mtE is expressed as mitochondrial volume, V_{mt} , and the
1092 mass of sample, m_X , is replaced by volume of sample, V_X , then D_{mtE} is the volume fraction of
1093 mitochondria in the sample.
1094 5 $mtE_X = mtE \cdot N_X^{-1} = C_{mtE} \cdot C_{NX}^{-1}$.
1095 6 O₂ can be replaced by other chemicals B to study different reactions, e.g., ATP, H₂O₂, or vesicular
1096 compartmental translocations, e.g., Ca²⁺.

- 1097 7 I_{O_2} and V are defined per instrument chamber as a system of constant volume (and constant
 1098 temperature), which may be closed or open. I_{O_2} is abbreviated for I_{rO_2} , *i.e.*, the metabolic or internal
 1099 O_2 flow of the chemical reaction r in which O_2 is consumed, hence the negative stoichiometric
 1100 number, $\nu_{O_2} = -1$. $I_{rO_2} = d_r n_{O_2} / dt \cdot \nu_{O_2}^{-1}$. If r includes all chemical reactions in which O_2 participates, then
 1101 $d_r n_{O_2} = dn_{O_2} - d_e n_{O_2}$, where dn_{O_2} is the change in the amount of O_2 in the instrument chamber and $d_e n_{O_2}$
 1102 is the amount of O_2 added externally to the system. At steady state, by definition $dn_{O_2} = 0$, hence $d_r n_{O_2}$
 1103 $= -d_e n_{O_2}$.
- 1104 8 J_{V,O_2} is an experimental variable, expressed per volume of the instrument chamber.
- 1105 9 $I_{O_2/X}$ is a physiological variable, depending on the size of entity X .
- 1106 10 There are many ways to normalize for a mitochondrial marker, that are used in different experimental
 1107 approaches: (1) $J_{O_2/mtE} = J_{V,O_2} \cdot C_{mtE}^{-1}$; (2) $J_{O_2/mtE} = J_{V,O_2} \cdot C_{mX}^{-1} \cdot D_{mtE}^{-1} = J_{O_2/mX} \cdot D_{mtE}^{-1}$; (3) $J_{O_2/mtE} =$
 1108 $J_{V,O_2} \cdot C_{NX}^{-1} \cdot mtE_X^{-1} = I_{O_2/X} \cdot mtE_X^{-1}$; (4) $J_{O_2/mtE} = I_{O_2} \cdot mtE^{-1}$. The mt-elemental unit [mtEU] varies between
 1109 different mt-markers.

1110

1111 **Sample concentration, C_{mX} :** Normalization for sample concentration is required to
 1112 report respiratory data. Considering a tissue or cells as the sample, X , the sample mass is m_X
 1113 [mg], which is frequently measured as wet or dry weight, W_w or W_d [mg], respectively, or as
 1114 amount of tissue or cell protein, m_{Protein} . In the case of permeabilized tissues, cells, and
 1115 homogenates, the sample concentration, $C_{mX} = m_X/V$ [$\text{g} \cdot \text{L}^{-1} = \text{mg} \cdot \text{mL}^{-1}$], is the mass of the
 1116 subsample of tissue that is transferred into the instrument chamber.

1117 **Mass-specific flux, $J_{O_2/mX}$:** Mass-specific flux is obtained by expressing respiration per
 1118 mass of sample, m_X [mg]. X is the type of sample—isolated mitochondria, tissue homogenate,
 1119 permeabilized fibres or cells. Volume-specific flux is divided by mass concentration of X , $J_{O_2/mX}$
 1120 $= J_{V,O_2}/C_{mX}$; or flow per cell is divided by mass per cell, $J_{O_2/mcell} = I_{O_2/cell}/M_{cell}$. If mass-specific
 1121 O_2 flux is constant and independent of sample size (expressed as mass), then there is no
 1122 interaction between the subsystems. A 1.5 mg and a 3.0 mg muscle sample respire at identical
 1123 mass-specific flux. Mass-specific O_2 flux, however, may change with the mass of a tissue
 1124 sample, cells or isolated mitochondria in the measuring chamber, in which the nature of the
 1125 interaction becomes an issue. Therefore, cell density must be optimized, particularly in
 1126 experiments carried out in wells, considering the confluency of the cell monolayer or clumps
 1127 of cells (Salabei *et al.* 2014).

1128

1129

Table 5. Sample types, X , abbreviations, and quantification.

Identity of sample	X	N_X	Mass ^a	Volume	mt-Marker
mitochondrial preparation	mt-prep	[x]	[kg]	[m ³]	[mtEU]
isolated mitochondria	imt		m_{mt}	V_{mt}	mtE
tissue homogenate	thom		m_{thom}		mtE_{thom}
permeabilized tissue	pti		m_{pti}		mtE_{pti}
permeabilized fibre	pfi		m_{pfi}		mtE_{pfi}
permeabilized cell	pce	N_{pce}	M_{pce}	V_{pce}	mtE_{pce}
cells ^b	cell	N_{cell}	M_{cell}	V_{cell}	mtE_{cell}
intact cell, viable cell	vce	N_{vce}	M_{vce}	V_{vce}	
dead cell	dce	N_{dce}	M_{dce}	V_{dce}	
organism	org	N_{org}	M_{org}	V_{org}	

1130

1131

1132

1133

1134

1135

1136

^a Instead of mass, the wet weight or dry weight is frequently stated, W_w or W_d .

m_X is mass of the sample [kg], M_X is mass of the object [$\text{kg} \cdot \text{x}^{-1}$].

^b Total cell count, $N_{cell} = N_{vce} + N_{dce}$

Number concentration, C_{NX} : C_{NX} is the experimental *number concentration* of sample X . In the case of cells or animals, *e.g.*, nematodes, $C_{NX} = N_X/V$ [$\text{x} \cdot \text{L}^{-1}$], where N_X is the number of cells or organisms in the chamber (Table 4).

1137 **Flow per object, $I_{O_2/X}$:** A special case of normalization is encountered in respiratory
 1138 studies with permeabilized (or intact) cells. If respiration is expressed per cell, the O_2 flow per
 1139 measurement system is replaced by the O_2 flow per cell, $I_{O_2/cell}$ (**Table 4**). O_2 flow can be
 1140 calculated from volume-specific O_2 flux, J_{V,O_2} [$\text{nmol}\cdot\text{s}^{-1}\cdot\text{L}^{-1}$] (per V of the measurement chamber
 1141 [L]), divided by the number concentration of cells, $C_{N_{cell}} = N_{cell}/V$ [$\text{cell}\cdot\text{L}^{-1}$], where N_{cell} is the
 1142 number of cells in the chamber. The total cell count is the sum of viable and dead cells, $N_{cell} =$
 1143 $N_{vce} + N_{dce}$ (**Table 5**). The cell viability index, $CVI = N_{vce}/N_{cell}$, is the ratio of viable cells (N_{vce} ;
 1144 before experimental permeabilization) per total cell count. After experimental permeabilization,
 1145 all cells are permeabilized, $N_{pce} = N_{cell}$. The cell viability index can be used to normalize
 1146 respiration for the number of cells that have been viable before experimental permeabilization,
 1147 $I_{O_2/vce} = I_{O_2/cell}/CVI$, considering that mitochondrial respiratory dysfunction in dead cells should
 1148 be eliminated as a confounding factor.

1149 Cellular O_2 flow can be compared between cells of identical size. To take into account
 1150 changes and differences in cell size, normalization is required to obtain cell size-specific or
 1151 mitochondrial marker-specific O_2 flux (Renner *et al.* 2003).

1152 The complexity changes when the sample is a whole organism studied as an experimental
 1153 model. The scaling law in respiratory physiology reveals a strong interaction of O_2 flow and
 1154 individual body mass of an organism, since *basal* metabolic rate (flow) does not increase
 1155 linearly with body mass, whereas *maximum* mass-specific O_2 flux, \dot{V}_{O_2max} or \dot{V}_{O_2peak} , is
 1156 approximately constant across a large range of individual body mass (Weibel and Hoppeler
 1157 2005), with individuals, breeds, and species deviating substantially from this relationship.
 1158 \dot{V}_{O_2peak} of human endurance athletes is 60 to 80 $\text{mL } O_2\cdot\text{min}^{-1}\cdot\text{kg}^{-1}$ body mass, converted to
 1159 $J_{O_2peak/M}$ of 45 to 60 $\text{nmol}\cdot\text{s}^{-1}\cdot\text{g}^{-1}$ (Gnaiger 2014; **Table 6**).

1160

1161 3.4. Normalization for mitochondrial content

1162

1163 Tissues can contain multiple cell populations that may have distinct mitochondrial
 1164 subtypes. Mitochondria undergo dynamic fission and fusion cycles, and can exist in multiple
 1165 stages and sizes that may be altered by a range of factors. The isolation of mitochondria (often
 1166 achieved through differential centrifugation) can therefore yield a subsample of the
 1167 mitochondrial types present in a tissue, depending on the isolation protocols utilized (*e.g.*,
 1168 centrifugation speed). This possible bias should be taken into account when planning
 1169 experiments using isolated mitochondria. Different sizes of mitochondria are enriched at
 1170 specific centrifugation speeds, which can be used strategically for isolation of mitochondrial
 1171 subpopulations.

1172 Part of the mitochondrial content of a tissue is lost during preparation of isolated
 1173 mitochondria. The fraction of isolated mitochondria obtained from a tissue sample is expressed
 1174 as mitochondrial recovery. At a high mitochondrial recovery the fraction of isolated
 1175 mitochondria is more representative of the total mitochondrial population than in preparations
 1176 characterized by low recovery. Determination of the mitochondrial recovery and yield is based
 1177 on measurement of the concentration of a mitochondrial marker in the stock of isolated
 1178 mitochondria, $C_{mtE,stock}$, and crude tissue homogenate, $C_{mtE,thom}$, which simultaneously provides
 1179 information on the specific mitochondrial density in the sample, D_{mtE} (**Table 4**).

1180 Normalization is a problematic subject; it is essential to consider the question of the study.
 1181 If the study aims at comparing tissue performance—such as the effects of a treatment on a
 1182 specific tissue, then normalization for tissue mass or protein content is appropriate. However,
 1183 if the aim is to find differences on mitochondrial function independent of mitochondrial density
 1184 (**Table 4**), then normalization to a mitochondrial marker is imperative (**Figure 7**). One cannot
 1185 assume that quantitative changes in various markers—such as mitochondrial proteins—
 1186 necessarily occur in parallel with one another. It should be established that the marker chosen
 1187 is not selectively altered by the performed treatment. In conclusion, the normalization must

1188 reflect the question under investigation to reach a satisfying answer. On the other hand, the goal
 1189 of comparing results across projects and institutions requires standardization on normalization
 1190 for entry into a databank.

1191 **Mitochondrial concentration, C_{mtE} , and mitochondrial markers:** Mitochondrial
 1192 organelles comprise a dynamic cellular reticulum in various states of fusion and fission. Hence,
 1193 the definition of an "amount" of mitochondria is often misconceived: mitochondria cannot be
 1194 counted reliably as a number of occurring elements. Therefore, quantification of the "amount"
 1195 of mitochondria depends on the measurement of chosen mitochondrial markers. 'Mitochondria
 1196 are the structural and functional elemental units of cell respiration' (Gnaiger 2014). The
 1197 quantity of a mitochondrial marker can reflect the amount of *mitochondrial elements*, mtE ,
 1198 expressed in various mitochondrial elemental units [mtEU] specific for each measured mt-
 1199 marker (**Table 4**). However, since mitochondrial quality may change in response to stimuli—
 1200 particularly in mitochondrial dysfunction and after exercise training (Pesta *et al.* 2011; Campos
 1201 *et al.* 2017) and during aging (Daum *et al.* 2013)—some markers can vary while others are
 1202 unchanged: (1) Mitochondrial volume and membrane area are structural markers, whereas
 1203 mitochondrial protein mass is frequently used as a marker for isolated mitochondria. (2)
 1204 Molecular and enzymatic mitochondrial markers (amounts or activities) can be selected as
 1205 matrix markers, *e.g.*, citrate synthase activity, mtDNA; mtIM-markers, *e.g.*, cytochrome *c*
 1206 oxidase activity, aa_3 content, cardiolipin, or mtOM-markers, *e.g.*, TOM20. (3) Extending the
 1207 measurement of mitochondrial marker enzyme activity to mitochondrial pathway capacity, ET-
 1208 or OXPHOS-capacity can be considered as an integrative functional mitochondrial marker.

1209 Depending on the type of mitochondrial marker, the mitochondrial elements, mtE , are
 1210 expressed in marker-specific units. Mitochondrial concentration in the measurement chamber
 1211 and the tissue of origin are quantified as (1) a quantity for normalization in functional analyses,
 1212 C_{mtE} , and (2) a physiological output that is the result of mitochondrial biogenesis and
 1213 degradation, D_{mtE} , respectively (**Table 4**). It is recommended, therefore, to distinguish
 1214 *experimental mitochondrial concentration*, $C_{mtE} = mtE/V$ and *physiological mitochondrial*
 1215 *density*, $D_{mtE} = mtE/m_X$. Then mitochondrial density is the amount of mitochondrial elements
 1216 per mass of tissue, which is a biological variable (**Figure 7**). The experimental variable is
 1217 mitochondrial density multiplied by sample mass concentration in the measuring chamber, C_{mtE}
 1218 $= D_{mtE} \cdot C_{mX}$, or mitochondrial content multiplied by sample number concentration, $C_{mtE} =$
 1219 $mtE_X \cdot C_{NX}$ (**Table 4**).

1220 **Mitochondria-specific flux, $J_{O_2/mtE}$:** Volume-specific metabolic O_2 flux depends on: (1)
 1221 the sample concentration in the volume of the instrument chamber, C_{mX} , or C_{NX} ; (2) the
 1222 mitochondrial density in the sample, $D_{mtE} = mtE/m_X$ or $mtE_X = mtE/N_X$; and (3) the specific
 1223 mitochondrial activity or performance per elemental mitochondrial unit, $J_{O_2/mtE} = J_{V,O_2}/C_{mtE}$
 1224 [$mol \cdot s^{-1} \cdot mtEU^{-1}$] (**Table 4**). Obviously, the numerical results for $J_{O_2/mtE}$ vary with the type of
 1225 mitochondrial marker chosen for measurement of mtE and $C_{mtE} = mtE/V$ [$mtEU \cdot m^{-3}$].

1226 1227 3.5. Evaluation of mitochondrial markers

1228
1229 Different methods are implicated in the quantification of mitochondrial markers and have
 1230 different strengths. Some problems are common for all mitochondrial markers, mtE : (1)
 1231 Accuracy of measurement is crucial, since even a highly accurate and reproducible
 1232 measurement of O_2 flux results in an inaccurate and noisy expression if normalized by a biased
 1233 and noisy measurement of a mitochondrial marker. This problem is acute in mitochondrial
 1234 respiration because the denominators used (the mitochondrial markers) are often small moieties
 1235 of which accurate and precise determination is difficult. This problem can be avoided when O_2
 1236 fluxes measured in substrate-uncoupler-inhibitor titration protocols are normalized for flux in
 1237 a defined respiratory reference state, which is used as an *internal* marker and yields flux control
 1238 ratios, *FCRs*. *FCRs* are independent of *externally* measured markers and, therefore, are

1239 statistically robust, considering the limitations of ratios in general (Jasienski and Bazzaz 1999).
1240 *FCRs* indicate qualitative changes of mitochondrial respiratory control, with highest
1241 quantitative resolution, separating the effect of mitochondrial density or concentration on $J_{O_2/mX}$
1242 and $I_{O_2/X}$ from that of function per elemental mitochondrial marker, $J_{O_2/mtE}$ (Pesta *et al.* 2011;
1243 Gnaiger 2014). (2) If mitochondrial quality does not change and only the amount of
1244 mitochondria varies as a determinant of mass-specific flux, any marker is equally qualified in
1245 principle; then in practice selection of the optimum marker depends only on the accuracy and
1246 precision of measurement of the mitochondrial marker. (3) If mitochondrial flux control ratios
1247 change, then there may not be any best mitochondrial marker. In general, measurement of
1248 multiple mitochondrial markers enables a comparison and evaluation of normalization for a
1249 variety of mitochondrial markers. Particularly during postnatal development, the activity of
1250 marker enzymes—such as cytochrome *c* oxidase and citrate synthase—follows different time
1251 courses (Drahota *et al.* 2004). Evaluation of mitochondrial markers in healthy controls is
1252 insufficient for providing guidelines for application in the diagnosis of pathological states and
1253 specific treatments.

1254 In line with the concept of the respiratory control ratio (Chance and Williams 1955a), the
1255 most readily used normalization is that of flux control ratios and flux control factors (Gnaiger
1256 2014). Selection of the state of maximum flux in a protocol as the reference state has the
1257 advantages of: (1) internal normalization; (2) statistical linearization of the response in the range
1258 of 0 to 1; and (3) consideration of maximum flux for integrating a large number of elemental
1259 steps in the OXPHOS- or ET-pathways. This reduces the risk of selecting a functional marker
1260 that is specifically altered by the treatment or pathology, yet increases the chance that the highly
1261 integrative pathway is disproportionately affected, *e.g.*, the OXPHOS- rather than ET-pathway
1262 in case of an enzymatic defect in the phosphorylation-pathway. In this case, additional
1263 information can be obtained by reporting flux control ratios based on a reference state which
1264 indicates stable tissue-mass specific flux. Stereological determination of mitochondrial content
1265 via two-dimensional transmission electron microscopy can have limitations due to the dynamics
1266 of mitochondrial size (Meinild Lundby *et al.* 2017). Accurate determination of three-
1267 dimensional volume by two-dimensional microscopy can be both time consuming and
1268 statistically challenging (Larsen *et al.* 2012).

1269 The validity of using mitochondrial marker enzymes (citrate synthase activity, Complex
1270 I–IV amount or activity) for normalization of flux is limited in part by the same factors that
1271 apply to flux control ratios. Strong correlations between various mitochondrial markers and
1272 citrate synthase activity (Reichmann *et al.* 1985; Boushel *et al.* 2007; Mogensen *et al.* 2007)
1273 are expected in a specific tissue of healthy subjects and in disease states not specifically
1274 targeting citrate synthase. Citrate synthase activity is acutely modifiable by exercise
1275 (Tonkonogi *et al.* 1997; Leek *et al.* 2001). Evaluation of mitochondrial markers related to a
1276 selected age and sex cohort cannot be extrapolated to provide recommendations for
1277 normalization in respirometric diagnosis of disease, in different states of development and
1278 ageing, different cell types, tissues, and species. mtDNA normalized to nDNA via qPCR is
1279 correlated to functional mitochondrial markers including OXPHOS- and ET-capacity in some
1280 cases (Puntschart *et al.* 1995; Wang *et al.* 1999; Menshikova *et al.* 2006; Boushel *et al.* 2007),
1281 but lack of such correlations have been reported (Menshikova *et al.* 2005; Schultz and Wiesner
1282 2000; Pesta *et al.* 2011). Several studies indicate a strong correlation between cardiolipin
1283 content and increase in mitochondrial function with exercise (Menshikova *et al.* 2005;
1284 Menshikova *et al.* 2007; Larsen *et al.* 2012; Faber *et al.* 2014), but it has not been evaluated as
1285 a general mitochondrial biomarker in disease.

1286
1287
1288
1289

1290 3.6. Conversion: units

1291

1292 Many different units have been used to report the O₂ consumption rate, OCR (**Table 6**).
 1293 *SI* base units provide the common reference to introduce the theoretical principles (**Figure 7**),
 1294 and are used with appropriately chosen *SI* prefixes to express numerical data in the most
 1295 practical format, with an effort towards unification within specific areas of application (**Table**
 1296 **7**). Reporting data in *SI* units—including the mole [mol], coulomb [C], joule [J], and second
 1297 [s]—should be encouraged, particularly by journals which propose the use of *SI* units.

1298

1299 **Table 6. Conversion of various units used in respirometry and**
 1300 **ergometry.** e^- is the number of electrons or reducing equivalents. z_B is the
 1301 charge number of entity B.
 1302

1 Unit		Multiplication factor	<i>SI</i> -unit	Note
ng.atom O·s ⁻¹	(2 e ⁻)	0.5	nmol O ₂ ·s ⁻¹	
ng.atom O·min ⁻¹	(2 e ⁻)	8.33	pmol O ₂ ·s ⁻¹	
natom O·min ⁻¹	(2 e ⁻)	8.33	pmol O ₂ ·s ⁻¹	
nmol O ₂ ·min ⁻¹	(4 e ⁻)	16.67	pmol O ₂ ·s ⁻¹	
nmol O ₂ ·h ⁻¹	(4 e ⁻)	0.2778	pmol O ₂ ·s ⁻¹	
mL O ₂ ·min ⁻¹ at STPD ^a		0.744	μmol O ₂ ·s ⁻¹	1
W = J/s at -470 kJ/mol O ₂		-2.128	μmol O ₂ ·s ⁻¹	
mA = mC·s ⁻¹	($z_{H^+} = 1$)	10.36	nmol H ⁺ ·s ⁻¹	2
mA = mC·s ⁻¹	($z_{O_2} = 4$)	2.59	nmol O ₂ ·s ⁻¹	2
nmol H ⁺ ·s ⁻¹	($z_{H^+} = 1$)	0.09649	mA	3
nmol O ₂ ·s ⁻¹	($z_{O_2} = 4$)	0.38594	mA	3

1303 1 At standard temperature and pressure dry (STPD: 0 °C = 273.15 K and 1 atm =
 1304 101.325 kPa = 760 mmHg), the molar volume of an ideal gas, V_m , and V_{m,O_2} is
 1305 22.414 and 22.392 L·mol⁻¹, respectively. Rounded to three decimal places, both
 1306 values yield the conversion factor of 0.744. For comparison at normal
 1307 temperature and pressure dry (NTPD: 20 °C), V_{m,O_2} is 24.038 L·mol⁻¹. Note that
 1308 the *SI* standard pressure is 100 kPa.

1309 2 The multiplication factor is $10^6/(z_B \cdot F)$.

1310 3 The multiplication factor is $z_B \cdot F/10^6$.

1311

1312 Although volume is expressed as m³ using the *SI* base unit, the litre [dm³] is a
 1313 conventional unit of volume for concentration and is used for most solution chemical kinetics.
 1314 If one multiplies $I_{O_2/cell}$ by C_{Ncell} , then the result will not only be the amount of O₂ [mol]
 1315 consumed per time [s⁻¹] in one litre [L⁻¹], but also the change in O₂ concentration per second
 1316 (for any volume of an ideally closed system). This is ideal for kinetic modeling as it blends with
 1317 chemical rate equations where concentrations are typically expressed in mol·L⁻¹ (Wagner *et al.*
 1318 2011). In studies of multinuclear cells—such as differentiated skeletal muscle cells—it is easy
 1319 to determine the number of nuclei but not the total number of cells. A generalized concept,
 1320 therefore, is obtained by substituting cells by nuclei as the sample entity. This does not hold,
 1321 however, for enucleated platelets.

1322 For studies of cells, we recommend that respiration be expressed, as far as possible, as:
 1323 (1) O₂ flux normalized for a mitochondrial marker, for separation of the effects of mitochondrial
 1324 quality and content on cell respiration (this includes *FCRs* as a normalization for a functional
 1325 mitochondrial marker); (2) O₂ flux in units of cell volume or mass, for comparison of respiration
 1326 of cells with different cell size (Renner *et al.* 2003) and with studies on tissue preparations, and

1327 (3) O₂ flow in units of attomole (10⁻¹⁸ mol) of O₂ consumed in a second by each cell
 1328 [amol·s⁻¹·cell⁻¹], numerically equivalent to [pmol·s⁻¹·10⁻⁶ cells]. This convention allows
 1329 information to be easily used when designing experiments in which O₂ flow must be considered.
 1330 For example, to estimate the volume-specific O₂ flux in an instrument chamber that would be
 1331 expected at a particular cell number concentration, one simply needs to multiply the flow per
 1332 cell by the number of cells per volume of interest. This provides the amount of O₂ [mol]
 1333 consumed per time [s⁻¹] per unit volume [L⁻¹]. At an O₂ flow of 100 amol·s⁻¹·cell⁻¹ and a cell
 1334 density of 10⁹ cells·L⁻¹ (10⁶ cells·mL⁻¹), the volume-specific O₂ flux is 100 nmol·s⁻¹·L⁻¹ (100
 1335 pmol·s⁻¹·mL⁻¹).
 1336
 1337

Table 7. Conversion of units with preservation of numerical values.

Name	Frequently used unit	Equivalent unit	Note
volume-specific flux, J_{V,O_2}	pmol·s ⁻¹ ·mL ⁻¹	nmol·s ⁻¹ ·L ⁻¹	1
	mmol·s ⁻¹ ·L ⁻¹	mol·s ⁻¹ ·m ⁻³	
cell-specific flow, $I_{O_2/cell}$	pmol·s ⁻¹ ·10 ⁻⁶ cells	amol·s ⁻¹ ·cell ⁻¹	2
	pmol·s ⁻¹ ·10 ⁻⁹ cells	zmol·s ⁻¹ ·cell ⁻¹	3
cell number concentration, C_{Nce}	10 ⁶ cells·mL ⁻¹	10 ⁹ cells·L ⁻¹	
mitochondrial protein concentration, C_{mtE}	0.1 mg·mL ⁻¹	0.1 g·L ⁻¹	
mass-specific flux, $J_{O_2/m}$	pmol·s ⁻¹ ·mg ⁻¹	nmol·s ⁻¹ ·g ⁻¹	4
catabolic power, P_k	μW·10 ⁻⁶ cells	pW·cell ⁻¹	1
volume	1,000 L	m ³ (1,000 kg)	
	L	dm ³ (kg)	
	mL	cm ³ (g)	
	μL	mm ³ (mg)	
	fL	μm ³ (pg)	5
amount of substance concentration	M = mol·L ⁻¹	mol·dm ⁻³	

1338

1339 1 pmol: picomole = 10⁻¹² mol4 nmol: nanomole = 10⁻⁹ mol1340 2 amol: attomole = 10⁻¹⁸ mol5 fL: femtolitre = 10⁻¹⁵ L1341 3 zmol: zeptomole = 10⁻²¹ mol

1342

1343 ET-capacity in human cell types including HEK 293, primary HUVEC and fibroblasts
 1344 ranges from 50 to 180 amol·s⁻¹·cell⁻¹, measured in intact cells in the noncoupled state (see
 1345 Gnaiger 2014). At 100 amol·s⁻¹·cell⁻¹ corrected for *Rox*, the current across the mt-membranes,
 1346 I_{H+e} , approximates 193 pA·cell⁻¹ or 0.2 nA per cell. See Rich (2003) for an extension of
 1347 quantitative bioenergetics from the molecular to the human scale, with a transmembrane proton
 1348 flux equivalent to 520 A in an adult at a catabolic power of -110 W. Modelling approaches
 1349 illustrate the link between protonmotive force and currents (Willis *et al.* 2016).

1350 We consider isolated mitochondria as powerhouses and proton pumps as molecular
 1351 machines to relate experimental results to energy metabolism of the intact cell. The cellular
 1352 P_»/O₂ based on oxidation of glycogen is increased by the glycolytic (fermentative) substrate-
 1353 level phosphorylation of 3 P_»/Glyc or 0.5 mol P_» for each mol O₂ consumed in the complete
 1354 oxidation of a mol glycosyl unit (Glyc). Adding 0.5 to the mitochondrial P_»/O₂ ratio of 5.4
 1355 yields a bioenergetic cell physiological P_»/O₂ ratio close to 6. Two NADH equivalents are
 1356 formed during glycolysis and transported from the cytosol into the mitochondrial matrix, either
 1357 by the malate-aspartate shuttle or by the glycerophosphate shuttle (**Figure 2A**) resulting in
 1358 different theoretical yields of ATP generated by mitochondria, the energetic cost of which
 1359 potentially must be taken into account. Considering also substrate-level phosphorylation in the
 1360 TCA cycle, this high P_»/O₂ ratio not only reflects proton translocation and OXPHOS studied

1361 in isolation, but integrates mitochondrial physiology with energy transformation in the living
1362 cell (Gnaiger 1993a).

1363

1364 4. Conclusions

1365

1366 MitoEAGLE can serve as a gateway to better diagnose mitochondrial respiratory defects
1367 linked to genetic variation, age-related health risks, sex-specific mitochondrial performance,
1368 lifestyle with its effects on degenerative diseases, and thermal and chemical environment. The
1369 present recommendations on coupling control states and rates, linked to the concept of the
1370 protonmotive force, are focused on studies with mitochondrial preparations. These will be
1371 extended in a series of reports on pathway control of mitochondrial respiration, respiratory
1372 states in intact cells, and harmonization of experimental procedures.

1373 OXPHOS analysis is based on the study of mitochondrial preparations complementary to
1374 bioenergetic investigations of intact cells and organisms—from model organisms to the human
1375 species including healthy and diseased persons (patients). Metabolic fluxes measured in defined
1376 coupling and pathway control states provide insights into the meaning of cellular and
1377 organismic respiration. An O₂ flux balance scheme illustrates the relationships and general
1378 definitions (**Figures 1 and 2**).

1379 Catabolic cell respiration is the process of exergonic and exothermic energy
1380 transformation in which scalar redox reactions are coupled to vectorial ion translocation across
1381 a semipermeable membrane, which separates the small volume of a bacterial cell or
1382 mitochondrion from the larger volume of its surroundings. The electrochemical exergy can be
1383 partially conserved in the phosphorylation of ADP to ATP or in ion pumping, or dissipated in
1384 an electrochemical short-circuit. Respiration is thus clearly distinguished from fermentation as
1385 the counterpart of cellular core energy metabolism. Respiration is separated in mitochondrial
1386 preparations from the interactions with the fermentative pathways of the intact cell.

1387 The optimal choice for expressing mitochondrial and cell respiration as O₂ flow per
1388 biological sample, and normalization for specific tissue-markers (volume, mass, protein) and
1389 mitochondrial markers (volume, protein, content, mtDNA, activity of marker enzymes,
1390 respiratory reference state) is guided by the scientific question under study. Interpretation of
1391 the data depends critically on appropriate normalization.

1392 We recommend for studies with mitochondrial preparations:

- 1393 • Normalization of respiratory rates should be provided as far as possible:
 - 1394 1. Biophysical normalization: on a per cell basis as O₂ flow; this may not be possible
1395 when dealing with coenocytic organisms or tissues without cross-walls separating
1396 individual cells (*e.g.*, filamentous fungi, muscle fibers)
 - 1397 2. Cellular normalization: per g protein; per cell- or tissue-mass as mass-specific O₂
1398 flux; per cell volume as cell volume-specific flux
 - 1399 3. Mitochondrial normalization: per mitochondrial marker as mt-specific flux.

1400 With information on cell size and the use of multiple normalizations, maximum potential
1401 information is available (Renner *et al.* 2003; Wagner *et al.* 2011; Gnaiger 2014).
1402 Reporting flow in a respiratory chamber [nmol·s⁻¹] is discouraged, since it restricts the
1403 analysis to intra-experimental comparison of relative (qualitative) differences.

- 1404 • Catabolic mitochondrial respiration is distinguished from residual oxygen consumption.
1405 Fluxes in mitochondrial coupling states should be, as far as possible, corrected for residual
1406 oxygen consumption.
- 1407 • Different mechanisms of uncoupling should be distinguished by defined terms. The
1408 tightness of coupling relates to these uncoupling mechanisms, whereas the coupling
1409 stoichiometry varies as a function the substrate type involved in ET-pathways with either
1410 three or two redox proton pumps operating in series. Separation of tightness of coupling
1411 from the pathway-dependent coupling stoichiometry is possible only when the substrate

- 1412 type undergoing oxidation remains the same for respiration in LEAK-, OXPHOS-, and
 1413 ET-states. In studies of the tightness of coupling, therefore, simple substrate-inhibitor
 1414 combinations should be applied to exclude a shift in substrate competition which may
 1415 occur when providing physiological substrate cocktails.
- 1416 • In studies of isolated mitochondria, the mitochondrial recovery and yield should be
 1417 reported. Experimental criteria for evaluation of purity versus integrity should be
 1418 considered. Mitochondrial markers—such as citrate synthase activity as an enzymatic
 1419 matrix marker—provide a link to the tissue of origin on the basis of calculating the
 1420 mitochondrial recovery, *i.e.*, the fraction of mitochondrial marker obtained from a unit
 1421 mass of tissue. Total mitochondrial protein is frequently applied as a mitochondrial
 1422 marker, which is restricted to isolated mitochondria.
 - 1423 • In studies of permeabilized cells, the viability of the cell culture or cell suspension of
 1424 origin should be reported. Normalization should be evaluated for total cell count or viable
 1425 cell count.
 - 1426 • Terms and symbols are summarized in **Table 8**. Their use will facilitate transdisciplinary
 1427 communication and support further developments towards a consistent theory of
 1428 bioenergetics and mitochondrial physiology. Technical terms related to and defined with
 1429 normal words can be used as index terms in databases, support the creation of ontologies
 1430 towards semantic information processing (MitoPedia), and help in communicating
 1431 analytical findings as impactful data-driven stories. ‘*Making data available without
 1432 making it understandable may be worse than not making it available at all*’ (National
 1433 Academies of Sciences, Engineering, and Medicine 2018). Success will depend on taking
 1434 next steps: (1) exhaustive text-mining considering Omics data and functional data; (2)
 1435 network analysis of Omics data with bioinformatics tools; (3) cross-validation with
 1436 distinct bioinformatics approaches; (4) correlation with functional data; (5) guidelines for
 1437 biological validation of network data. This is a call to carefully contribute to FAIR
 1438 principles (Findable, Accessible, Interoperable, Reusable) for the sharing of scientific
 1439 data.

1441 **Table 8. Terms, symbols, and units.**

1442 Term	1443 Symbol	1444 Unit	1445 Links and comments
1446 alternative quinol oxidase	1447 AOX		1448 Figure 2B
1449 amount of substance B	n_B	1450 [mol]	
1451 ATP yield per O_2	$Y_{P\gg O_2}$		1452 $P\gg O_2$ ratio measured in any respiratory 1453 state
1454 catabolic reaction	k		1455 Figure 1 and 3
1456 catabolic respiration	J_{kO_2}	1457 <i>varies</i>	1458 Figure 1 and 3
1459 cell number	N_{cell}	1460 [x]	1461 Table 5; $N_{cell} = N_{vce} + N_{dce}$
1462 cell respiration	J_{rO_2}	1463 <i>varies</i>	1464 Figure 1
1465 cell viability index	CVI		1466 $CVI = N_{vce}/N_{cell} = 1 - N_{dce}/N_{cell}$
1467 Complexes I to IV	CI to CIV		1468 respiratory ET Complexes; Figure 2B
1469 concentration of substance B	$c_B = n_B \cdot V^{-1}$; [B]	1470 [mol·m ⁻³]	1471 Box 2
1472 dead cell number	N_{dce}	1473 [x]	1474 Table 5; non-viable cells, loss of plasma 1475 membrane barrier function
1476 electron transfer system	ETS		1477 Figure 2B, Figure 5; state
1478 flow, for substance B	I_B	1479 [mol·s ⁻¹]	1480 system-related extensive quantity; 1481 Figure 7
1482 flux, for substance B	J_B	1483 <i>varies</i>	1484 size-specific quantity; Figure 7
1485 inorganic phosphate	P_i		1486 Figure 3
1487 intact cell number, viable cell number	N_{vce}	1488 [x]	1489 Table 5; viable cells, intact of plasma 1490 membrane barrier function
1491 LEAK	LEAK		1492 Table 1, Figure 5; state
1493 mass of sample X	m_X	1494 [kg]	1495 Table 4

1469	mass of entity X	M_X	[kg]	mass of object X ; Table 4
1470	MITOCARTA			https://www.broadinstitute.org/scientific-community/science/programs/metabolic-disease-program/publications/mitocarta/mitocarta-in-0
1471				
1472				
1473				
1474				
1475	MitoPedia			http://www.bioblast.at/index.php/MitoPedia
1476	mitochondria or mitochondrial	mt		Box 1
1477	mitochondrial DNA	mtDNA		Box 1
1478	mitochondrial concentration	$C_{mtE} = mtE \cdot V^{-1}$	[mtEU·m ⁻³]	Table 4
1479	mitochondrial content	$mtE_X = mtE \cdot N_X^{-1}$	[mtEU·x ⁻¹]	Table 4
1480	mitochondrial elemental unit	mtEU	<i>varies</i>	Table 4, specific units for mt-marker
1481	mitochondrial inner membrane	mtIM		Figure 2; MIM is widely used; the first M is replaced by mt; Box 1
1482				
1483	mitochondrial outer membrane	mtOM		Figure 2; MOM is widely used; the first M is replaced by mt; Box 1
1484				
1485	mitochondrial recovery	Y_{mtE}		fraction of <i>mtE</i> recovered in sample from the tissue of origin
1486				
1487	mitochondrial yield	$Y_{mtE/m}$		$Y_{mtE/m} = Y_{mtE} \cdot D_{mtE}$
1488	negative	neg		Figure 3
1489	number concentration of X	C_{NX}	[x·m ⁻³]	Table 4
1490	number of entities X	N_X	[x]	Table 4, Figure 7
1491	number of entity B	N_B	[x]	Table 4
1492	oxidative phosphorylation	OXPPOS		Table 1, Figure 5; state
1493	oxygen concentration	$c_{O_2} = n_{O_2} \cdot V^{-1}$; [O ₂]	[mol·m ⁻³]	Section 3.2
1494	oxygen flux, in reaction r	J_{rO_2}	<i>varies</i>	Figure 1
1495	permeabilized cell number	N_{pce}	[x]	Table 5; experimental permeabilization of plasma membrane; $N_{pce} = N_{cell}$
1496				
1497	phosphorylation of ADP to ATP	P»		Section 2.2
1498	positive	pos		Figure 3
1499	proton in the negative compartment	H ⁺ _{neg}		Figure 3
1500	proton in the positive compartment	H ⁺ _{pos}		Figure 3
1501	rate of electron transfer in ET state	E		ET-capacity; Table 1
1502	rate of LEAK respiration	L		Table 1
1503	rate of oxidative phosphorylation	P		OXPPOS capacity; Table 1
1504	rate of residual oxygen consumption	ROX		Table 1, Figure 1
1505	residual oxygen consumption	ROX		Table 1; state
1506	respiratory supercomplex	SC I _n III _n IV _n		Box 1; supramolecular assemblies composed of variable copy numbers (n) of CI, CIII and CIV
1507				
1508				
1509	specific mitochondrial density	$D_{mtE} = mtE \cdot m_X^{-1}$	[mtEU·kg ⁻¹]	Table 4
1510	volume	V	[m ⁻³]	Table 7
1511	weight, dry weight	W_d	[kg]	used as mass of sample X ; Figure 7
1512	weight, wet weight	W_w	[kg]	used as mass of sample X ; Figure 7
1513				

1514

1515 Acknowledgements

1516 We thank M. Beno for management assistance. This publication is based upon work from COST
1517 Action CA15203 MitoEAGLE, supported by COST (European Cooperation in Science and
1518 Technology), and K-Regio project MitoFit (E.G.).

1519

1520 **Competing financial interests:** E.G. is founder and CEO of Oroboros Instruments, Innsbruck,
1521 Austria.

1522

1523 References

1524

1525 Altmann R (1894) Die Elementarorganismen und ihre Beziehungen zu den Zellen. Zweite vermehrte Auflage.
1526 Verlag Von Veit & Comp, Leipzig:160 pp.

- 1527 Beard DA (2005) A biophysical model of the mitochondrial respiratory system and oxidative phosphorylation.
1528 PLoS Comput Biol 1(4):e36.
- 1529 Benda C (1898) Weitere Mitteilungen über die Mitochondria. Verh Dtsch Physiol Ges:376-83.
- 1530 Birkedal R, Laasmaa M, Vendelin M (2014) The location of energetic compartments affects energetic
1531 communication in cardiomyocytes. Front Physiol 5:376.
- 1532 Breton S, Beaupré HD, Stewart DT, Hoeh WR, Blier PU (2007) The unusual system of doubly uniparental
1533 inheritance of mtDNA: isn't one enough? Trends Genet 23:465-74.
- 1534 Brown GC (1992) Control of respiration and ATP synthesis in mammalian mitochondria and cells. Biochem J
1535 284:1-13.
- 1536 Calvo SE, Klauser CR, Mootha VK (2016) MitoCarta2.0: an updated inventory of mammalian mitochondrial
1537 proteins. Nucleic Acids Research 44:D1251-7.
- 1538 Calvo SE, Julien O, Clauser KR, Shen H, Kamer KJ, Wells JA, Mootha VK (2017) Comparative analysis of
1539 mitochondrial N-termini from mouse, human, and yeast. Mol Cell Proteomics 16:512-23.
- 1540 Campos JC, Queliconi BB, Bozi LHM, Bechara LRG, Dourado PMM, Andres AM, Jannig PR, Gomes KMS,
1541 Zambelli VO, Rocha-Resende C, Guatimosim S, Brum PC, Mochly-Rosen D, Gottlieb RA, Kowaltowski AJ,
1542 Ferreira JCB (2017) Exercise reestablishes autophagic flux and mitochondrial quality control in heart failure.
1543 Autophagy 13:1304-317.
- 1544 Canton M, Luvisetto S, Schmehl I, Azzone GF (1995) The nature of mitochondrial respiration and
1545 discrimination between membrane and pump properties. Biochem J 310:477-81.
- 1546 Carrico C, Meyer JG, He W, Gibson BW, Verdin E (2018) The mitochondrial acylome emerges: proteomics,
1547 regulation by Sirtuins, and metabolic and disease implications. Cell Metab 27:497-512.
- 1548 Chance B, Williams GR (1955a) Respiratory enzymes in oxidative phosphorylation. I. Kinetics of oxygen
1549 utilization. J Biol Chem 217:383-93.
- 1550 Chance B, Williams GR (1955b) Respiratory enzymes in oxidative phosphorylation: III. The steady state. J Biol
1551 Chem 217:409-27.
- 1552 Chance B, Williams GR (1955c) Respiratory enzymes in oxidative phosphorylation. IV. The respiratory chain. J
1553 Biol Chem 217:429-38.
- 1554 Chance B, Williams GR (1956) The respiratory chain and oxidative phosphorylation. Adv Enzymol Relat Subj
1555 Biochem 17:65-134.
- 1556 Cobb LJ, Lee C, Xiao J, Yen K, Wong RG, Nakamura HK, Mehta HH, Gao Q, Ashur C, Huffman DM, Wan J,
1557 Muzumdar R, Barzilai N, Cohen P (2016) Naturally occurring mitochondrial-derived peptides are age-
1558 dependent regulators of apoptosis, insulin sensitivity, and inflammatory markers. Aging (Albany NY) 8:796-
1559 809.
- 1560 Cohen ER, Cvitas T, Frey JG, Holmström B, Kuchitsu K, Marquardt R, Mills I, Pavese F, Quack M, Stohner J,
1561 Strauss HL, Takami M, Thor HL (2008) Quantities, units and symbols in physical chemistry, IUPAC Green
1562 Book, 3rd Edition, 2nd Printing, IUPAC & RSC Publishing, Cambridge.
- 1563 Cooper H, Hedges LV, Valentine JC, eds (2009) The handbook of research synthesis and meta-analysis. Russell
1564 Sage Foundation.
- 1565 Coopersmith J (2010) Energy, the subtle concept. The discovery of Feynman's blocks from Leibnitz to Einstein.
1566 Oxford University Press:400 pp.
- 1567 Cummins J (1998) Mitochondrial DNA in mammalian reproduction. Rev Reprod 3:172-82.
- 1568 Dai Q, Shah AA, Garde RV, Yonish BA, Zhang L, Medvitz NA, Miller SE, Hansen EL, Dunn CN, Price TM
1569 (2013) A truncated progesterone receptor (PR-M) localizes to the mitochondrion and controls cellular
1570 respiration. Mol Endocrinol 27:741-53.
- 1571 Daum B, Walter A, Horst A, Osiewacz HD, Kühlbrandt W (2013) Age-dependent dissociation of ATP synthase
1572 dimers and loss of inner-membrane cristae in mitochondria. Proc Natl Acad Sci U S A 110:15301-6.
- 1573 Divakaruni AS, Brand MD (2011) The regulation and physiology of mitochondrial proton leak. Physiology
1574 (Bethesda) 26:192-205.
- 1575 Doerrier C, Garcia-Souza LF, Krumschnabel G, Wohlfarter Y, Mészáros AT, Gnaiger E (2018) High-Resolution
1576 Fluorescence Respirometry and OXPHOS protocols for human cells, permeabilized fibres from small biopsies of
1577 muscle, and isolated mitochondria. Methods Mol Biol 1782 (Palmeira CM, Moreno AJ, eds): Mitochondrial
1578 Bioenergetics, 978-1-4939-7830-4.
- 1579 Doskey CM, van 't Erve TJ, Wagner BA, Buettner GR (2015) Moles of a substance per cell is a highly
1580 informative dosing metric in cell culture. PLOS ONE 10:e0132572.
- 1581 Drahotová Z, Milerová M, Stieglarová A, Houstek J, Ostádal B (2004) Developmental changes of cytochrome *c*
1582 oxidase and citrate synthase in rat heart homogenate. Physiol Res 53:119-22.
- 1583 Duarte FV, Palmeira CM, Rolo AP (2014) The role of microRNAs in mitochondria: small players acting wide.
1584 Genes (Basel) 5:865-86.
- 1585 Ernster L, SCHATZ G (1981) Mitochondria: a historical review. J Cell Biol 91:227s-55s.
- 1586 Estabrook RW (1967) Mitochondrial respiratory control and the polarographic measurement of ADP:O ratios.
1587 Methods Enzymol 10:41-7.

- 1588 Faber C, Zhu ZJ, Castellino S, Wagner DS, Brown RH, Peterson RA, Gates L, Barton J, Bickett M, Hagerty L,
 1589 Kimbrough C, Sola M, Bailey D, Jordan H, Elangbam CS (2014) Cardiolipin profiles as a potential
 1590 biomarker of mitochondrial health in diet-induced obese mice subjected to exercise, diet-restriction and
 1591 ephedrine treatment. *J Appl Toxicol* 34:1122-9.
- 1592 Fell D (1997) Understanding the control of metabolism. Portland Press.
- 1593 Garlid KD, Beavis AD, Ratkje SK (1989) On the nature of ion leaks in energy-transducing membranes. *Biochim*
 1594 *Biophys Acta* 976:109-20.
- 1595 Garlid KD, Semrad C, Zinchenko V. Does redox slip contribute significantly to mitochondrial respiration? In:
 1596 Schuster S, Rigoulet M, Ouhabi R, Mazat J-P, eds (1993) Modern trends in biothermokinetics. Plenum Press,
 1597 New York, London:287-93.
- 1598 Gerö D, Szabo C (2016) Glucocorticoids suppress mitochondrial oxidant production via upregulation of
 1599 uncoupling protein 2 in hyperglycemic endothelial cells. *PLoS One* 11:e0154813.
- 1600 Gnaiger E. Efficiency and power strategies under hypoxia. Is low efficiency at high glycolytic ATP production a
 1601 paradox? In: Surviving Hypoxia: Mechanisms of Control and Adaptation. Hochachka PW, Lutz PL, Sick T,
 1602 Rosenthal M, Van den Thillart G, eds (1993a) CRC Press, Boca Raton, Ann Arbor, London, Tokyo:77-109.
- 1603 Gnaiger E (1993b) Nonequilibrium thermodynamics of energy transformations. *Pure Appl Chem* 65:1983-2002.
- 1604 Gnaiger E (2001) Bioenergetics at low oxygen: dependence of respiration and phosphorylation on oxygen and
 1605 adenosine diphosphate supply. *Respir Physiol* 128:277-97.
- 1606 Gnaiger E (2009) Capacity of oxidative phosphorylation in human skeletal muscle. New perspectives of
 1607 mitochondrial physiology. *Int J Biochem Cell Biol* 41:1837-45.
- 1608 Gnaiger E (2014) Mitochondrial pathways and respiratory control. An introduction to OXPHOS analysis. 4th ed.
 1609 Mitochondr Physiol Network 19.12. Oroboros MiPNet Publications, Innsbruck:80 pp.
- 1610 Gnaiger E, Méndez G, Hand SC (2000) High phosphorylation efficiency and depression of uncoupled respiration
 1611 in mitochondria under hypoxia. *Proc Natl Acad Sci USA* 97:11080-5.
- 1612 Greggio C, Jha P, Kulkarni SS, Lagarrigue S, Broskey NT, Boutant M, Wang X, Conde Alonso S, Ofori E,
 1613 Auwerx J, Cantó C, Amati F (2017) Enhanced respiratory chain supercomplex formation in response to
 1614 exercise in human skeletal muscle. *Cell Metab* 25:301-11.
- 1615 Hinkle PC (2005) P/O ratios of mitochondrial oxidative phosphorylation. *Biochim Biophys Acta* 1706:1-11.
- 1616 Hofstadter DR (1979) Gödel, Escher, Bach: An eternal golden braid. A metaphorical fugue on minds and
 1617 machines in the spirit of Lewis Carroll. Harvester Press:499 pp.
- 1618 Illaste A, Laasmaa M, Peterson P, Vendelin M (2012) Analysis of molecular movement reveals latticelike
 1619 obstructions to diffusion in heart muscle cells. *Biophys J* 102:739-48.
- 1620 Jasienski M, Bazzaz FA (1999) The fallacy of ratios and the testability of models in biology. *Oikos* 84:321-26.
- 1621 Jepihina N, Beraud N, Sepp M, Birkedal R, Vendelin M (2011) Permeabilized rat cardiomyocyte response
 1622 demonstrates intracellular origin of diffusion obstacles. *Biophys J* 101:2112-21.
- 1623 Klepinin A, Ounpuu L, Guzun R, Chekulayev V, Timohhina N, Tepp K, Shevchuk I, Schlattner U, Kaambre T
 1624 (2016) Simple oxygraphic analysis for the presence of adenylate kinase 1 and 2 in normal and tumor cells. *J*
 1625 *Bioenerg Biomembr* 48:531-48.
- 1626 Klingenberg M (2017) UCP1 - A sophisticated energy valve. *Biochimie* 134:19-27.
- 1627 Koit A, Shevchuk I, Ounpuu L, Klepinin A, Chekulayev V, Timohhina N, Tepp K, Puurand M, Truu L, Heck K,
 1628 Valvere V, Guzun R, Kaambre T (2017) Mitochondrial respiration in human colorectal and breast cancer
 1629 clinical material is regulated differently. *Oxid Med Cell Longev* 1372640.
- 1630 Komlódi T, Tretter L (2017) Methylene blue stimulates substrate-level phosphorylation catalysed by succinyl-
 1631 CoA ligase in the citric acid cycle. *Neuropharmacology* 123:287-98.
- 1632 Lane N (2005) Power, sex, suicide: mitochondria and the meaning of life. Oxford University Press:354 pp.
- 1633 Larsen S, Nielsen J, Neigaard Nielsen C, Nielsen LB, Wibrand F, Stride N, Schroder HD, Boushel RC, Helge
 1634 JW, Dela F, Hey-Mogensen M (2012) Biomarkers of mitochondrial content in skeletal muscle of healthy
 1635 young human subjects. *J Physiol* 590:3349-60.
- 1636 Lee C, Zeng J, Drew BG, Sallam T, Martin-Montalvo A, Wan J, Kim SJ, Mehta H, Hevener AL, de Cabo R,
 1637 Cohen P (2015) The mitochondrial-derived peptide MOTS-c promotes metabolic homeostasis and reduces
 1638 obesity and insulin resistance. *Cell Metab* 21:443-54.
- 1639 Lee SR, Kim HK, Song IS, Youm J, Dizon LA, Jeong SH, Ko TH, Heo HJ, Ko KS, Rhee BD, Kim N, Han J
 1640 (2013) Glucocorticoids and their receptors: insights into specific roles in mitochondria. *Prog Biophys Mol*
 1641 *Biol* 112:44-54.
- 1642 Leek BT, Mudaliar SR, Henry R, Mathieu-Costello O, Richardson RS (2001) Effect of acute exercise on citrate
 1643 synthase activity in untrained and trained human skeletal muscle. *Am J Physiol Regul Integr Comp Physiol*
 1644 280:R441-7.
- 1645 Lemieux H, Blier PU, Gnaiger E (2017) Remodeling pathway control of mitochondrial respiratory capacity by
 1646 temperature in mouse heart: electron flow through the Q-junction in permeabilized fibers. *Sci Rep* 7:2840.
- 1647 Lenaz G, Tioli G, Falasca AI, Genova ML (2017) Respiratory supercomplexes in mitochondria. In: Mechanisms
 1648 of primary energy transduction in biology. M Wikstrom (ed) Royal Society of Chemistry Publishing, London,
 1649 UK:296-337.

- 1650 Liu S, Roellig DM, Guo Y, Li N, Frace MA, Tang K, Zhang L, Feng Y, Xiao L (2016) Evolution of mitosome
1651 metabolism and invasion-related proteins in *Cryptosporidium*. BMC Genomics 17:1006.
- 1652 Margulis L (1970) Origin of eukaryotic cells. New Haven: Yale University Press.
- 1653 Meinild Lundby AK, Jacobs RA, Gehrig S, de Leur J, Hauser M, Bonne TC, Flück D, Dandanell S, Kirk N,
1654 Kaech A, Ziegler U, Larsen S, Lundby C (2018) Exercise training increases skeletal muscle mitochondrial
1655 volume density by enlargement of existing mitochondria and not de novo biogenesis. Acta Physiol 222,
1656 e12905.
- 1657 Menshikova EV, Ritov VB, Fairfull L, Ferrell RE, Kelley DE, Goodpaster BH (2006) Effects of exercise on
1658 mitochondrial content and function in aging human skeletal muscle. J Gerontol A Biol Sci Med Sci 61:534-
1659 40.
- 1660 Menshikova EV, Ritov VB, Ferrell RE, Azuma K, Goodpaster BH, Kelley DE (2007) Characteristics of skeletal
1661 muscle mitochondrial biogenesis induced by moderate-intensity exercise and weight loss in obesity. J Appl
1662 Physiol (1985) 103:21-7.
- 1663 Menshikova EV, Ritov VB, Toledo FG, Ferrell RE, Goodpaster BH, Kelley DE (2005) Effects of weight loss
1664 and physical activity on skeletal muscle mitochondrial function in obesity. Am J Physiol Endocrinol Metab
1665 288:E818-25.
- 1666 Miller GA (1991) The science of words. Scientific American Library New York:276 pp.
- 1667 Mitchell P (1961) Coupling of phosphorylation to electron and hydrogen transfer by a chemi-osmotic type of
1668 mechanism. Nature 191:144-8.
- 1669 Mitchell P (2011) Chemiosmotic coupling in oxidative and photosynthetic phosphorylation. Biochim Biophys
1670 Acta Bioenergetics 1807:1507-38.
- 1671 Mogensen M, Sahlin K, Fernström M, Glintborg D, Vind BF, Beck-Nielsen H, Højlund K (2007) Mitochondrial
1672 respiration is decreased in skeletal muscle of patients with type 2 diabetes. Diabetes 56:1592-9.
- 1673 Mohr PJ, Phillips WD (2015) Dimensionless units in the SI. Metrologia 52:40-7.
- 1674 Moreno M, Giacco A, Di Munno C, Goglia F (2017) Direct and rapid effects of 3,5-diiodo-L-thyronine (T2).
1675 Mol Cell Endocrinol 7207:30092-8.
- 1676 Morrow RM, Picard M, Derbeneva O, Leipzig J, McManus MJ, Gouspillou G, Barbat-Artigas S, Dos Santos C,
1677 Hepple RT, Murdock DG, Wallace DC (2017) Mitochondrial energy deficiency leads to hyperproliferation of
1678 skeletal muscle mitochondria and enhanced insulin sensitivity. Proc Natl Acad Sci U S A 114:2705-10.
- 1679 Murley A, Nunnari J (2016) The emerging network of mitochondria-organelle contacts. Mol Cell 61:648-53.
- 1680 National Academies of Sciences, Engineering, and Medicine (2018) International coordination for science data
1681 infrastructure: Proceedings of a workshop—in brief. Washington, DC: The National Academies Press. doi:
1682 <https://doi.org/10.17226/25015>.
- 1683 Palmfeldt J, Bross P (2017) Proteomics of human mitochondria. Mitochondrion 33:2-14.
- 1684 Paradies G, Paradies V, De Benedictis V, Ruggiero FM, Petrosillo G (2014) Functional role of cardiolipin in
1685 mitochondrial bioenergetics. Biochim Biophys Acta 1837:408-17.
- 1686 Pesta D, Gnaiger E (2012) High-Resolution Respirometry. OXPHOS protocols for human cells and
1687 permeabilized fibres from small biopsies of human muscle. Methods Mol Biol 810:25-58.
- 1688 Pesta D, Hoppel F, Macek C, Messner H, Faulhaber M, Kobel C, Parson W, Burtcher M, Schocke M, Gnaiger
1689 E (2011) Similar qualitative and quantitative changes of mitochondrial respiration following strength and
1690 endurance training in normoxia and hypoxia in sedentary humans. Am J Physiol Regul Integr Comp Physiol
1691 301:R1078–87.
- 1692 Price TM, Dai Q (2015) The role of a mitochondrial progesterone receptor (PR-M) in progesterone action.
1693 Semin Reprod Med 33:185-94.
- 1694 Puchowicz MA, Varnes ME, Cohen BH, Friedman NR, Kerr DS, Hoppel CL (2004) Oxidative phosphorylation
1695 analysis: assessing the integrated functional activity of human skeletal muscle mitochondria – case studies.
1696 Mitochondrion 4:377-85. Puntschart A, Claassen H, Jostardt K, Hoppeler H, Billeter R (1995) mRNAs of
1697 enzymes involved in energy metabolism and mtDNA are increased in endurance-trained athletes. Am J
1698 Physiol 269:C619-25.
- 1699 Quiros PM, Mottis A, Auwerx J (2016) Mitonuclear communication in homeostasis and stress. Nat Rev Mol
1700 Cell Biol 17:213-26.
- 1701 Rackham O, Mercer TR, Filipovska A (2012) The human mitochondrial transcriptome and the RNA-binding
1702 proteins that regulate its expression. WIREs RNA 3:675–95.
- 1703 Reichmann H, Hoppeler H, Mathieu-Costello O, von Bergen F, Pette D (1985) Biochemical and ultrastructural
1704 changes of skeletal muscle mitochondria after chronic electrical stimulation in rabbits. Pflugers Arch 404:1-
1705 9.
- 1706 Renner K, Amberger A, Konwalinka G, Gnaiger E (2003) Changes of mitochondrial respiration, mitochondrial
1707 content and cell size after induction of apoptosis in leukemia cells. Biochim Biophys Acta 1642:115-23.
- 1708 Rice DW, Alverson AJ, Richardson AO, Young GJ, Sanchez-Puerta MV, Munzinger J, Barry K, Boore JL,
1709 Zhang Y, dePamphilis CW, Knox EB, Palmer JD (2016) Horizontal transfer of entire genomes via
1710 mitochondrial fusion in the angiosperm *Amborella*. Science 342:1468-73.
- 1711 Rich P (2003) Chemiosmotic coupling: The cost of living. Nature 421:583.

- 1712 Rostovtseva TK, Sheldon KL, Hassanzadeh E, Monge C, Saks V, Bezrukov SM, Sackett DL (2008) Tubulin
1713 binding blocks mitochondrial voltage-dependent anion channel and regulates respiration. *Proc Natl Acad Sci*
1714 *USA* 105:18746-51.
- 1715 Rustin P, Parfait B, Chretien D, Bourgeron T, Djouadi F, Bastin J, Rötig A, Munnich A (1996) Fluxes of
1716 nicotinamide adenine dinucleotides through mitochondrial membranes in human cultured cells. *J Biol Chem*
1717 271:14785-90.
- 1718 Saks VA, Veksler VI, Kuznetsov AV, Kay L, Sikk P, Tiivel T, Tranqui L, Olivares J, Winkler K, Wiedemann F,
1719 Kunz WS (1998) Permeabilised cell and skinned fiber techniques in studies of mitochondrial function in
1720 vivo. *Mol Cell Biochem* 184:81-100.
- 1721 Salabei JK, Gibb AA, Hill BG (2014) Comprehensive measurement of respiratory activity in permeabilized cells
1722 using extracellular flux analysis. *Nat Protoc* 9:421-38.
- 1723 Sazanov LA (2015) A giant molecular proton pump: structure and mechanism of respiratory complex I. *Nat Rev*
1724 *Mol Cell Biol* 16:375-88.
- 1725 Schneider TD (2006) Claude Shannon: biologist. The founder of information theory used biology to formulate
1726 the channel capacity. *IEEE Eng Med Biol Mag* 25:30-3.
- 1727 Schönfeld P, Dymkowska D, Wojtczak L (2009) Acyl-CoA-induced generation of reactive oxygen species in
1728 mitochondrial preparations is due to the presence of peroxisomes. *Free Radic Biol Med* 47:503-9.
- 1729 Schultz J, Wiesner RJ (2000) Proliferation of mitochondria in chronically stimulated rabbit skeletal muscle--
1730 transcription of mitochondrial genes and copy number of mitochondrial DNA. *J Bioenerg Biomembr* 32:627-
1731 34.
- 1732 Speijer D (2016) Being right on Q: shaping eukaryotic evolution. *Biochem J* 473:4103-27.
- 1733 Sugiura A, Mattie S, Prudent J, McBride HM (2017) Newly born peroxisomes are a hybrid of mitochondrial and
1734 ER-derived pre-peroxisomes. *Nature* 542:251-4.
- 1735 Simson P, Jepihhina N, Laasmaa M, Peterson P, Birkedal R, Vendelin M (2016) Restricted ADP movement in
1736 cardiomyocytes: Cytosolic diffusion obstacles are complemented with a small number of open mitochondrial
1737 voltage-dependent anion channels. *J Mol Cell Cardiol* 97:197-203.
- 1738 Stucki JW, Ineichen EA (1974) Energy dissipation by calcium recycling and the efficiency of calcium transport
1739 in rat-liver mitochondria. *Eur J Biochem* 48:365-75.
- 1740 Tonkonogi M, Harris B, Sahlin K (1997) Increased activity of citrate synthase in human skeletal muscle after a
1741 single bout of prolonged exercise. *Acta Physiol Scand* 161:435-6.
- 1742 Torralba D, Baixauli F, Sánchez-Madrid F (2016) Mitochondria know no boundaries: mechanisms and functions
1743 of intercellular mitochondrial transfer. *Front Cell Dev Biol* 4:107. eCollection 2016.
- 1744 Vamecq J, Schepers L, Parmentier G, Mannaerts GP (1987) Inhibition of peroxisomal fatty acyl-CoA oxidase by
1745 antimycin A. *Biochem J* 248:603-7.
- 1746 Waczulikova I, Habodaszova D, Cagalinec M, Ferko M, Ulicna O, Mateasik A, Sikurova L, Ziegelhöffer A
1747 (2007) Mitochondrial membrane fluidity, potential, and calcium transients in the myocardium from acute
1748 diabetic rats. *Can J Physiol Pharmacol* 85:372-81.
- 1749 Wagner BA, Venkataraman S, Buettner GR (2011) The rate of oxygen utilization by cells. *Free Radic Biol Med*
1750 51:700-712.
- 1751 Wang H, Hiatt WR, Barstow TJ, Brass EP (1999) Relationships between muscle mitochondrial DNA content,
1752 mitochondrial enzyme activity and oxidative capacity in man: alterations with disease. *Eur J Appl Physiol*
1753 *Occup Physiol* 80:22-7.
- 1754 Watt IN, Montgomery MG, Runswick MJ, Leslie AG, Walker JE (2010) Bioenergetic cost of making an
1755 adenosine triphosphate molecule in animal mitochondria. *Proc Natl Acad Sci U S A* 107:16823-7.
- 1756 Weibel ER, Hoppeler H (2005) Exercise-induced maximal metabolic rate scales with muscle aerobic capacity. *J*
1757 *Exp Biol* 208:1635-44.
- 1758 White DJ, Wolff JN, Pierson M, Gemmell NJ (2008) Revealing the hidden complexities of mtDNA inheritance.
1759 *Mol Ecol* 17:4925-42.
- 1760 Wikström M, Hummer G (2012) Stoichiometry of proton translocation by respiratory complex I and its
1761 mechanistic implications. *Proc Natl Acad Sci U S A* 109:4431-6.
- 1762 Williams EG, Wu Y, Jha P, Dubuis S, Blattmann P, Argmann CA, Houten SM, Amariuta T, Wolski W,
1763 Zamboni N, Aebersold R, Auwerx J (2016) Systems proteomics of liver mitochondria function. *Science* 352
1764 (6291):aad0189
- 1765 Willis WT, Jackman MR, Messer JI, Kuzmiak-Glancy S, Glancy B (2016) A simple hydraulic analog model of
1766 oxidative phosphorylation. *Med Sci Sports Exerc* 48:990-1000.
- 1767